Debye Lecture 9

Multi-Component Nanocrystal Assemblies

C. B. Murray

Designing Nanoscale Materials

Lecture Series by 2004 Debye Institute Professor

Christopher B. Murray

IBM Research

Ornstein Laboratory 166

Office phone 253 2227

cbmurray@alum.mit.edu

Semiconductor Quantum Dot Arrays

Glassy QD Solids

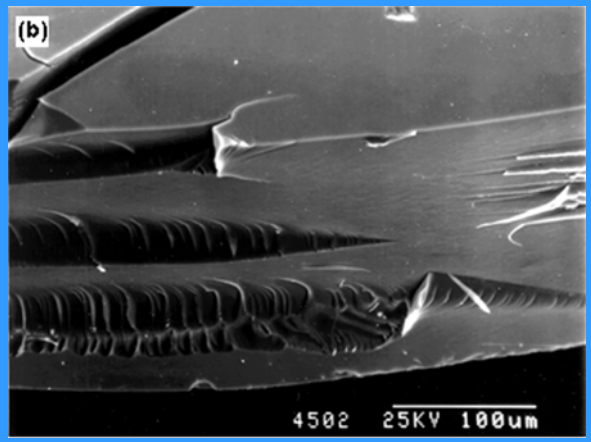

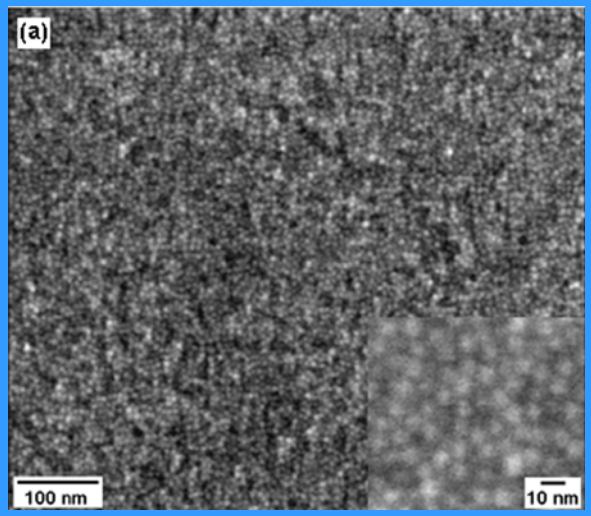

Crystalline QD Solids

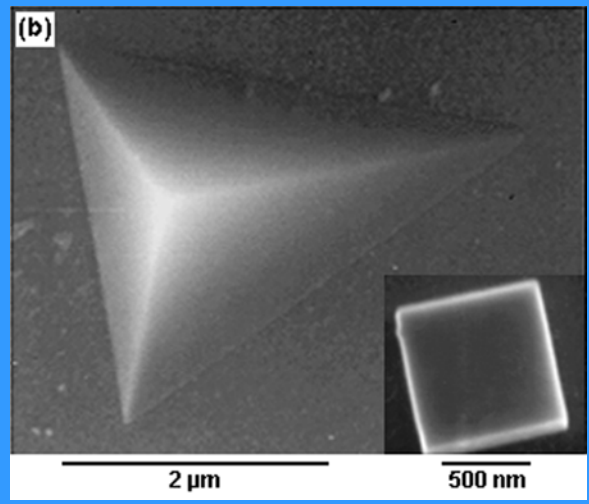

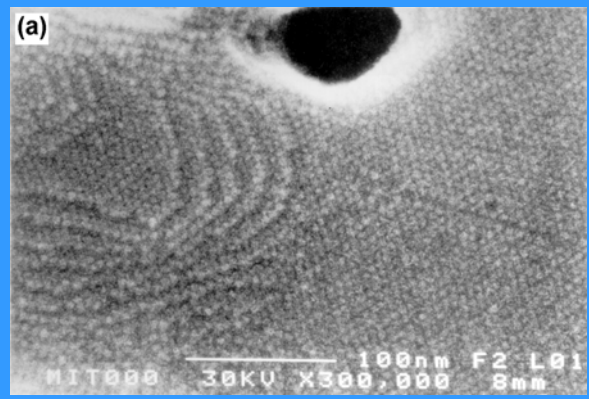

Most of the work in this tutorial can be found in:

C. B. Murray, C. R. Kagan, M. G. Bawendi, Ann. Rev. Mat. Sci.

C. R. Kagan, Thesis, MIT (1996).

C. B. Murray, Thesis, MIT (1995).

Absorption and Fluorescence of CdSe Quantum Dot Solids

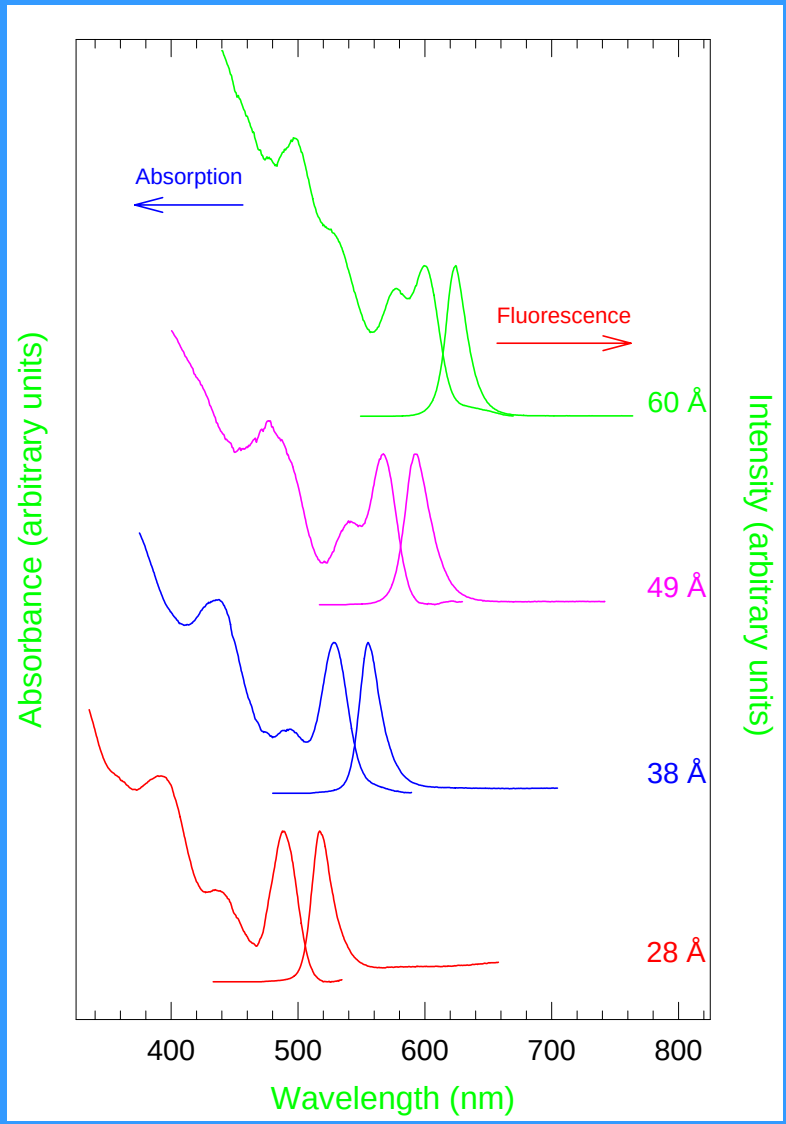

Quantum Dot Solids

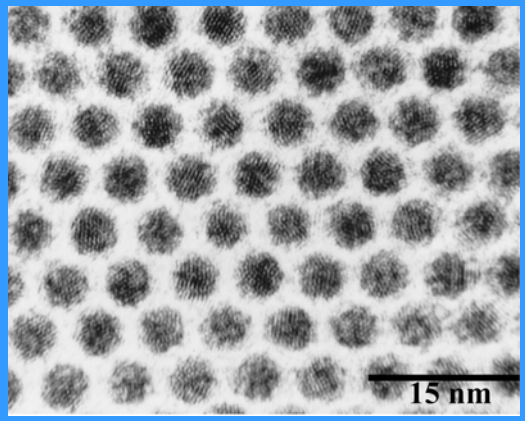

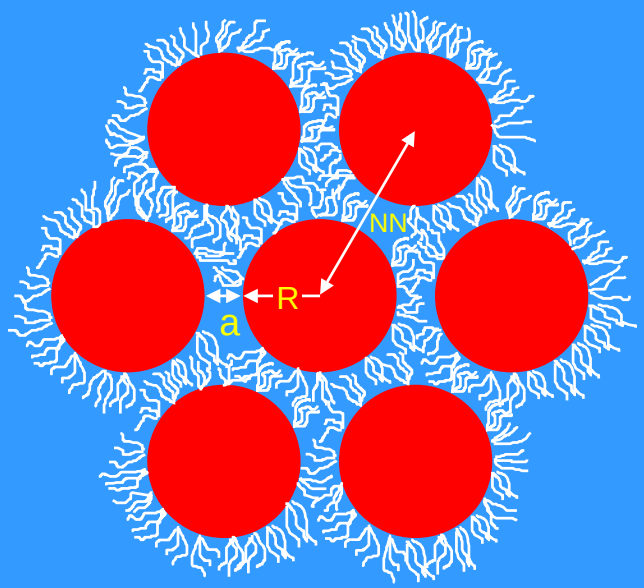

Particle Size and Nearest Neighbor Distance from Small Angle X-ray Scattering

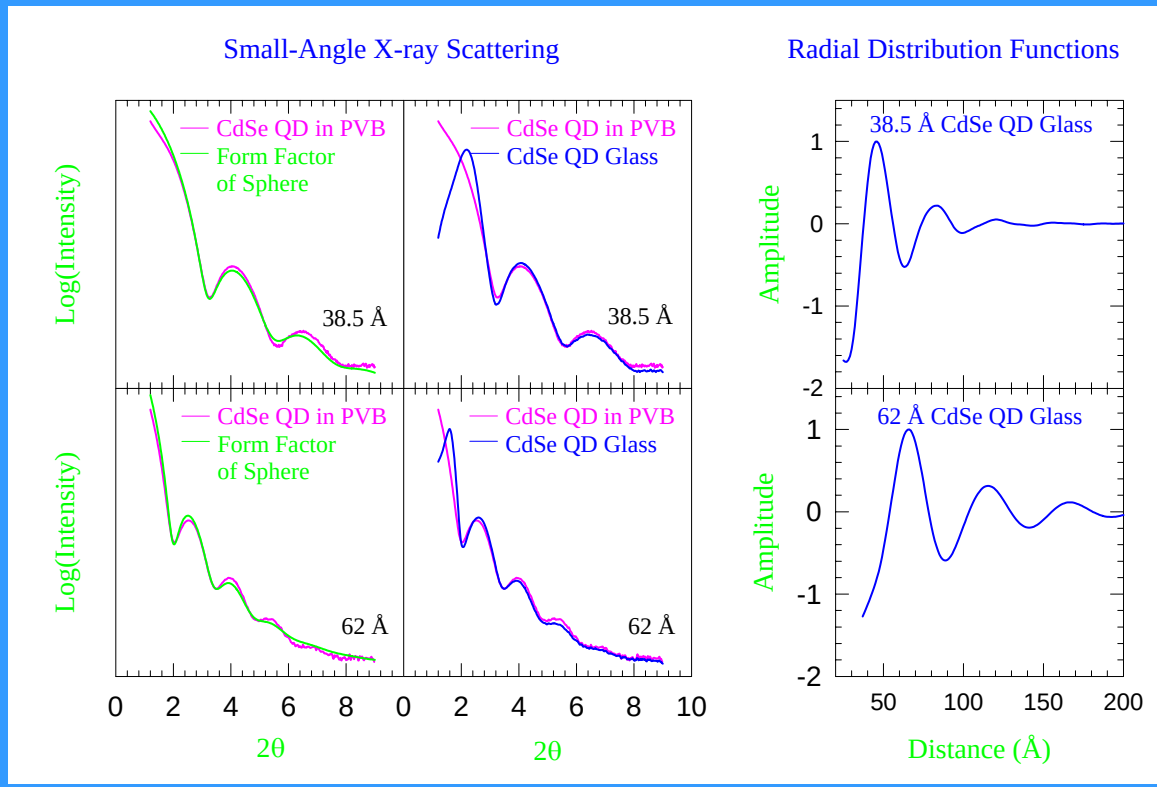

R

NN

Mixed QD Solids

Ordered

Glassy

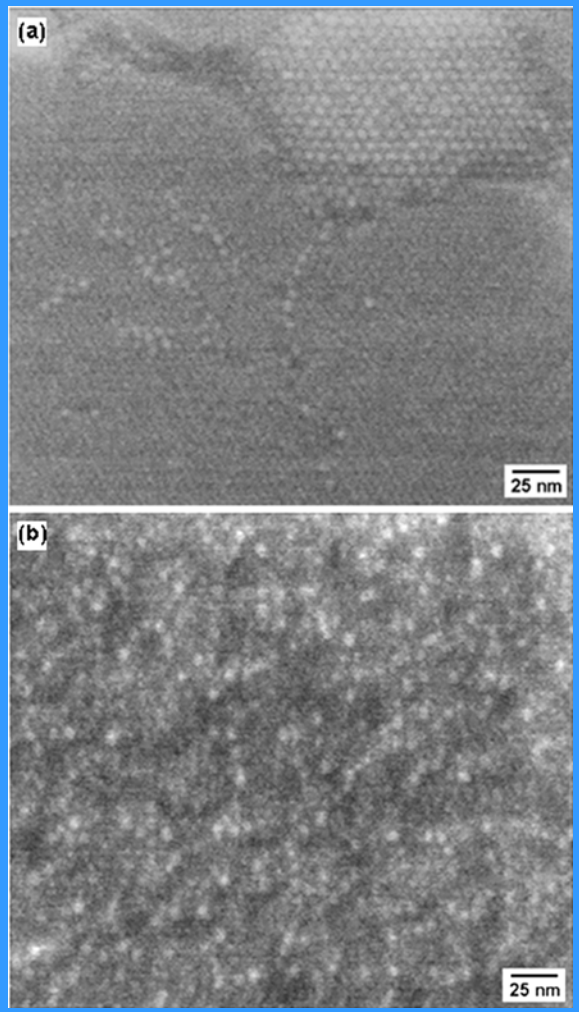

Didn’t satisy radius ratio rules to form ordered intermetallic phases

18% 38.5 Å/82% 62Å CdSe QDs

Photoconductivity in Quantum Dot Solids

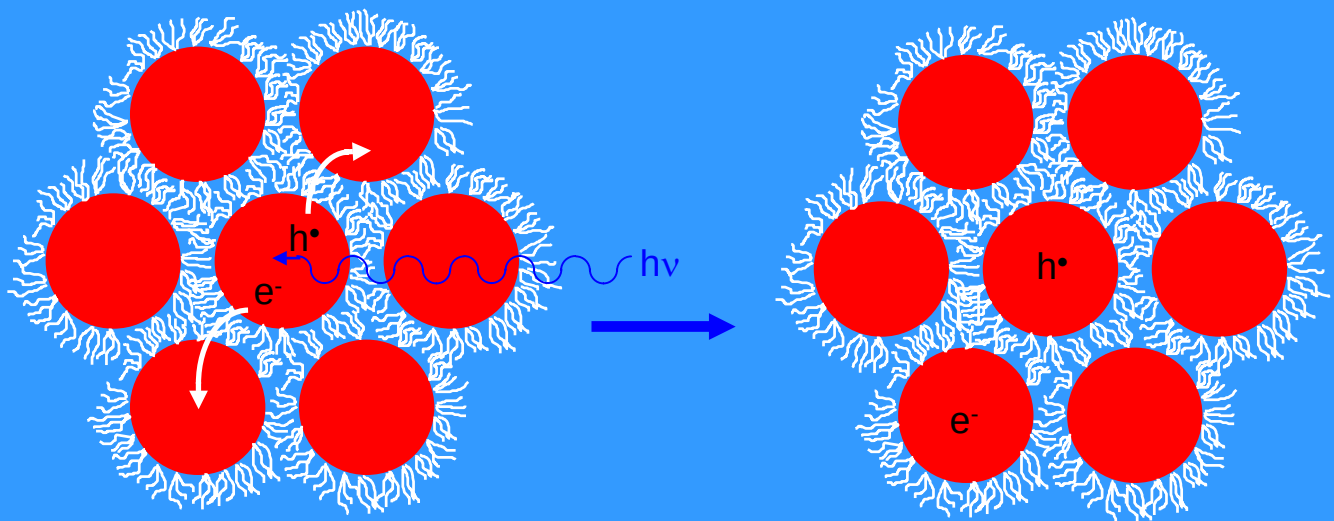

Charge Neutral

2 Charged QDs

C. A. Leatherdale, C. R. Kagan, N. Y. Morgan, S. A. Empedocles, M. A. Kastner, M. G. Bawendi, Phys. Rev. B, **62**, 2669 (2000).

Spectral Response of Photoconductivity

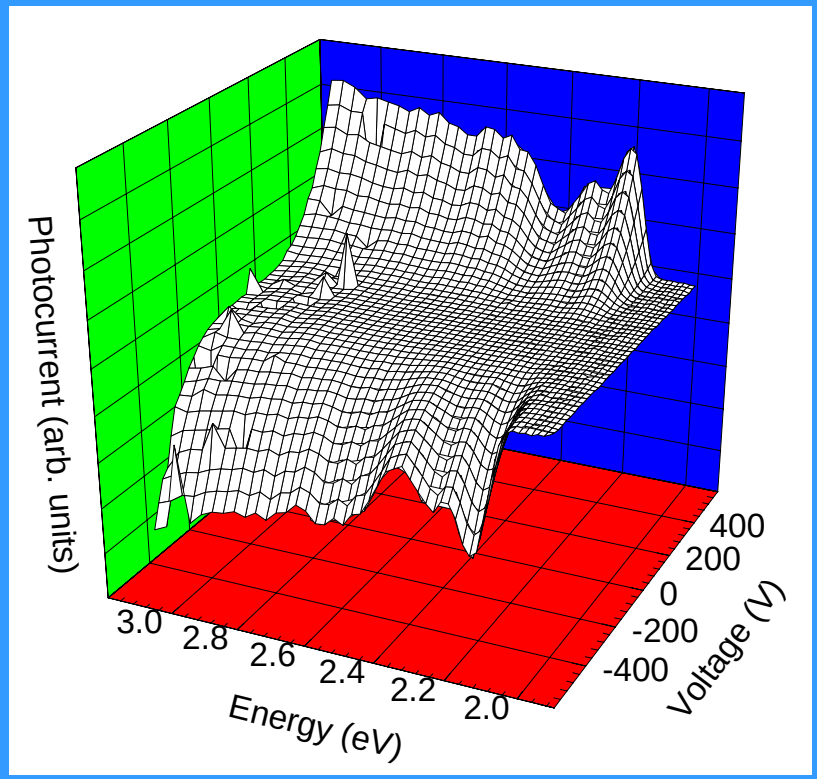

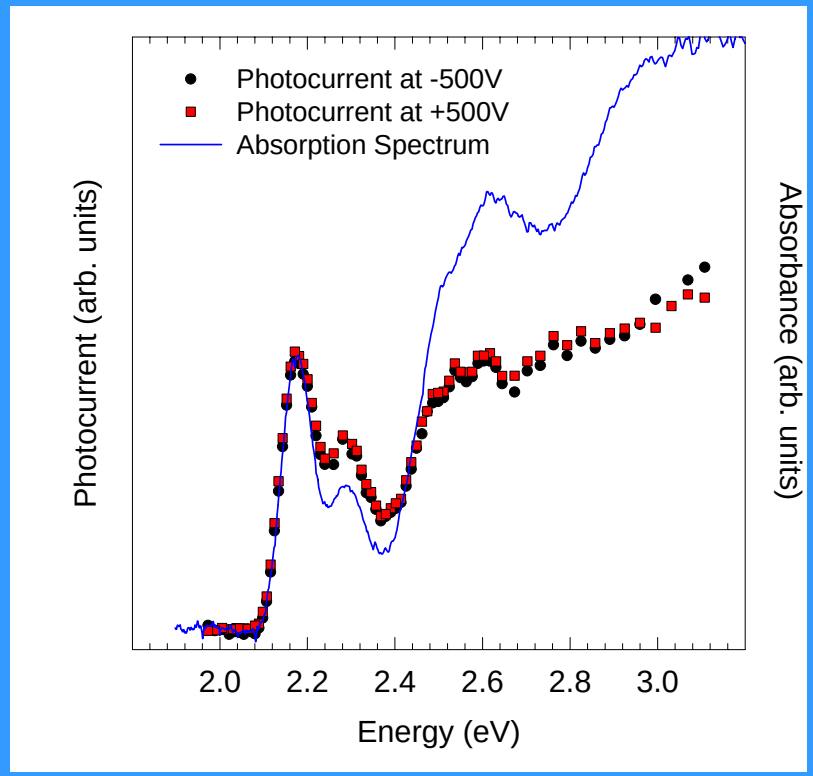

Size and Interparticle Distance Dependence of Photoconductivity

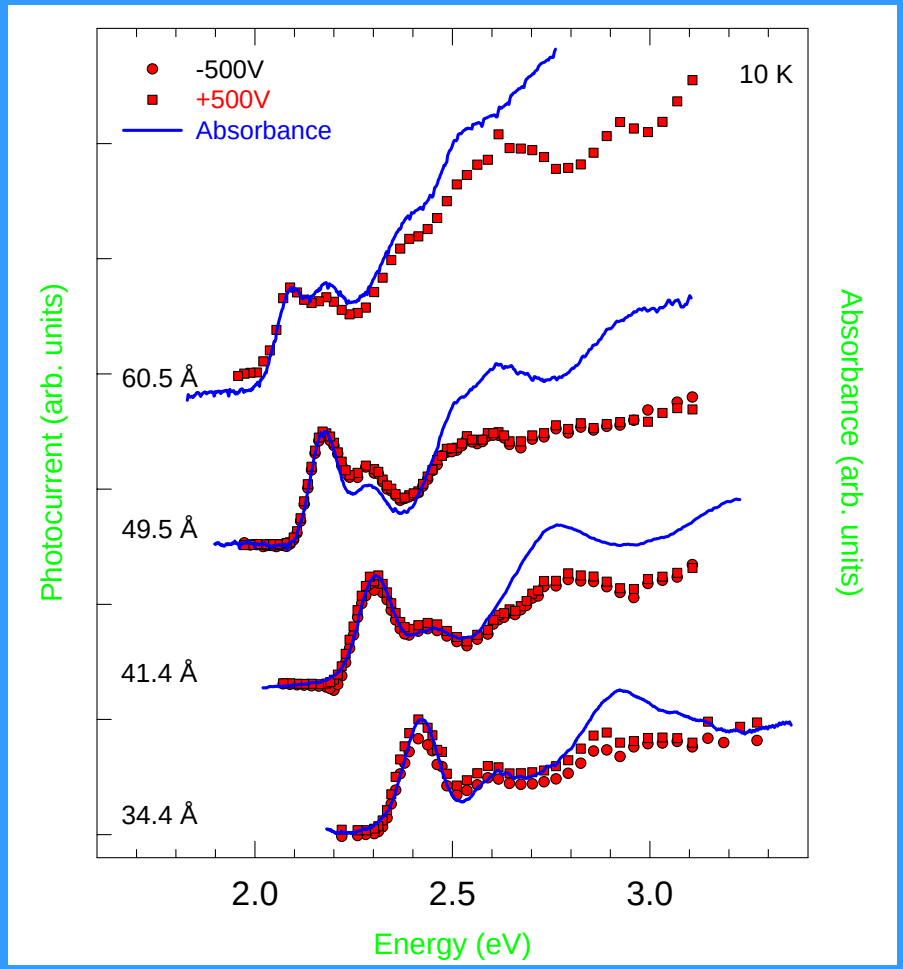

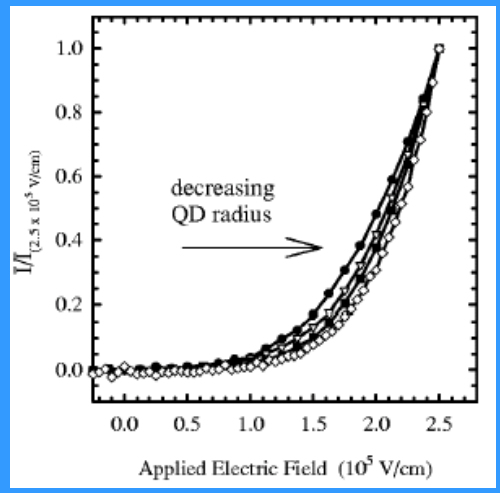

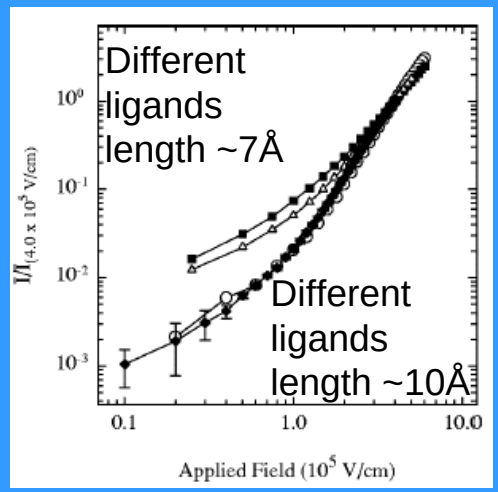

- Spectral response maps the size-dependent, discrete electronic states of QDs
- Photocarriers thermalize to lowest excited state before being separated

Increased energy required to overcome binding energy with decreasing QD size

Temperature Dependence of the Photoconductivity

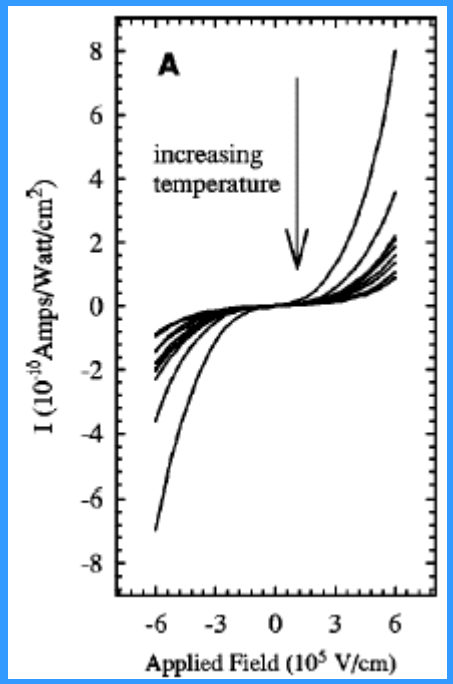

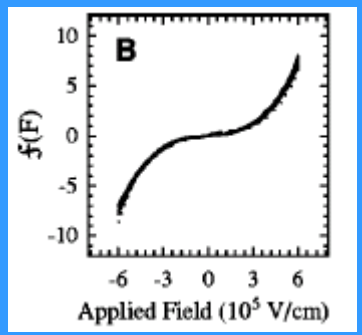

Scale I-V curves to nearly universal curve

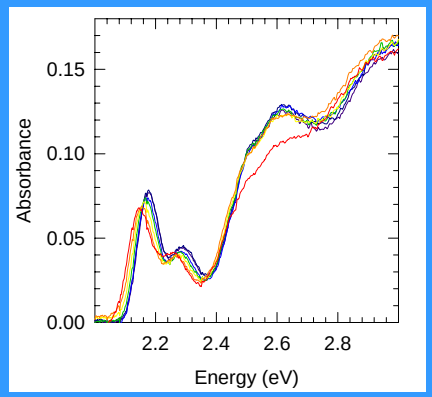

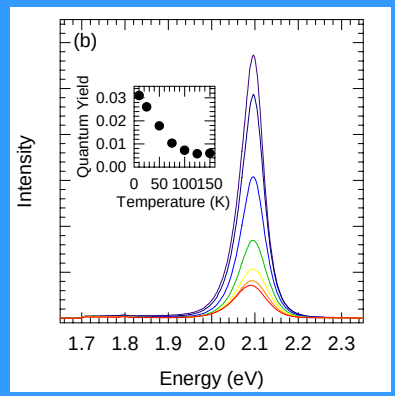

Temperature dependence of the Quantum Yield

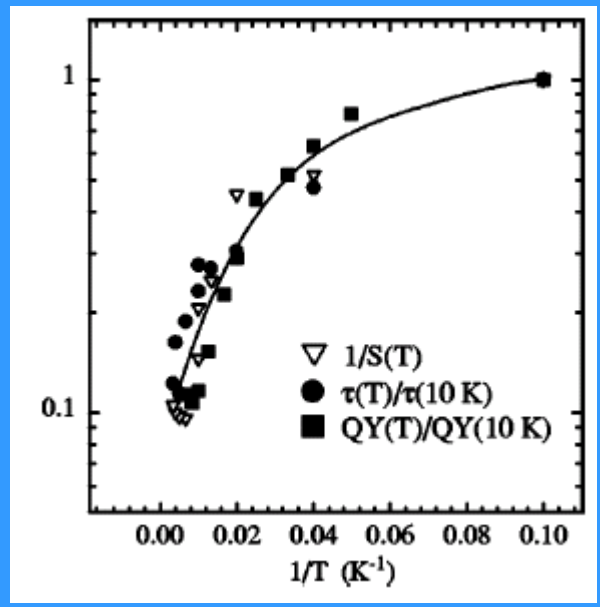

Decrease in photocurrent and the decrease in lifetime and Quantum Yield have the same temperature dependence

Fluorescence Quenching

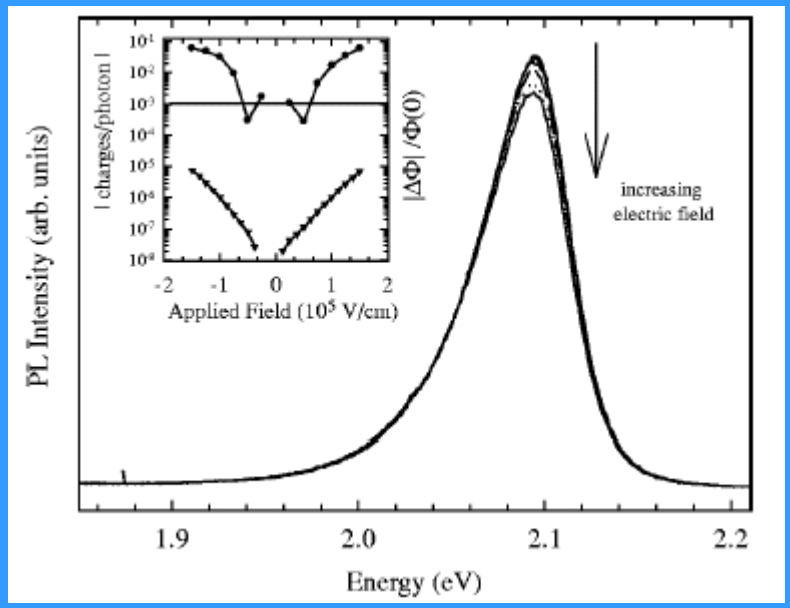

Well passivated QDs

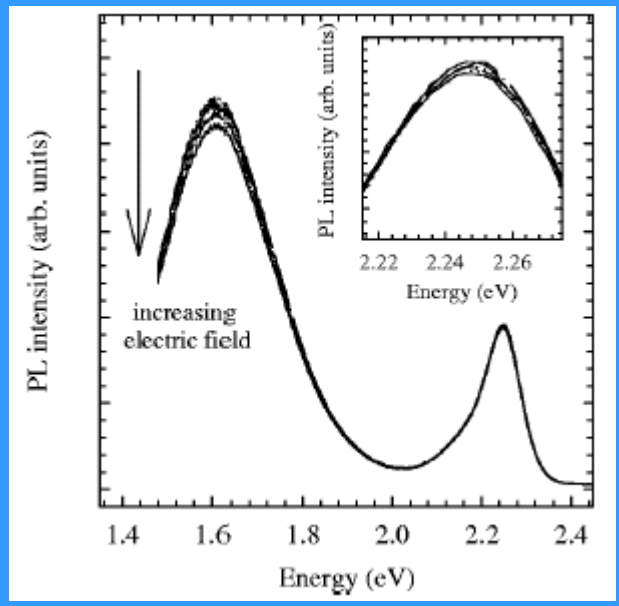

Poorly passivated QDs
Deep trap emission quenched at lower fields than band edge emission

Quenching not observed in PL of isolated QDs in applied field

Quenching not directly proportional to charge separation efficiency as free charges in film may quench PL by Auger process

Measureable quenching possible sign of free charges in film

Charge Separation versus Geminate Recombination

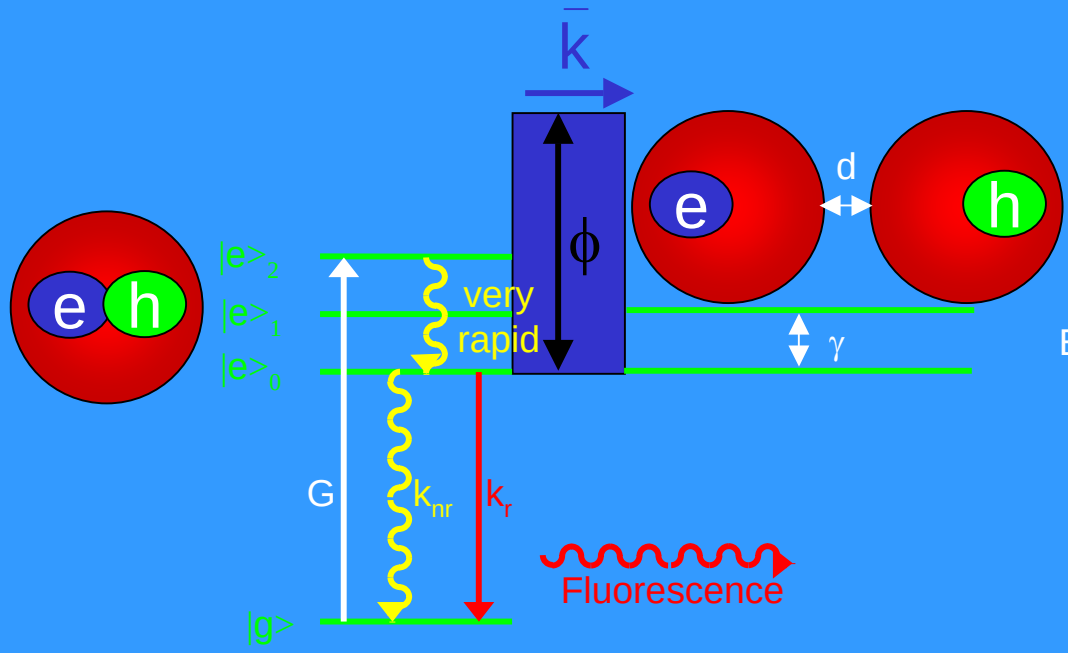

Energy offset of initial and final states

Efficiency of Charge Separation

$$\eta(E,T) = \frac{\bar{k}(E,T)}{\underbrace{\bar{k}(E,T) + k_{nr}(T) + k_r(T)}}$$

assume weakly field-dependent

For $\bar{k}(E,T) << k_r(T) + k_{nr}(T)$

$$\eta(E,T) = \tau(T)\bar{k}(E,T)$$

Overcome:
- Coulomb attraction between e^- and h
- Charging Energy

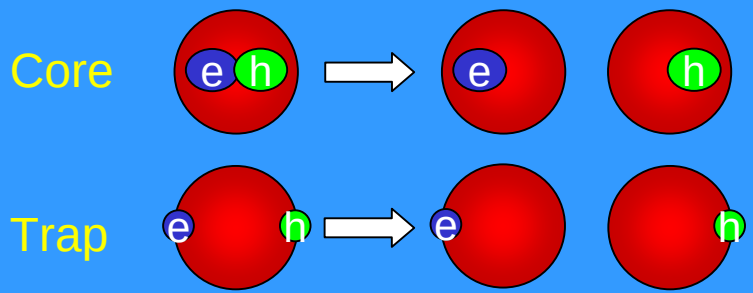

Dipole-Dipole Interaction

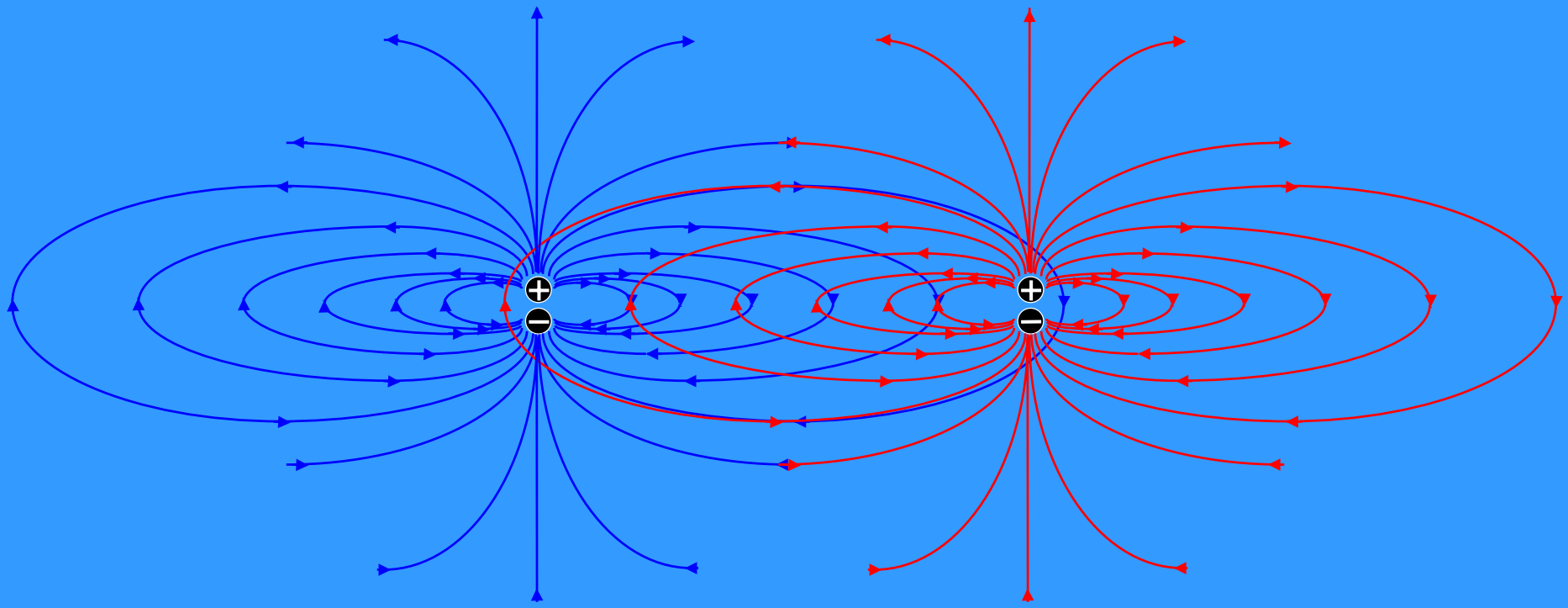

Excited Donor

Unexcited Acceptor

Field Created by
Transition Dipole of Donor

Transfer Energy

Interaction Energy

Induce Transition
Field Created by
Transition Dipole of Acceptor

Couple via Mutual Radiation Fields
Created by Transition Dipoles

Coulombic Interaction

Electronic Energy Transfer

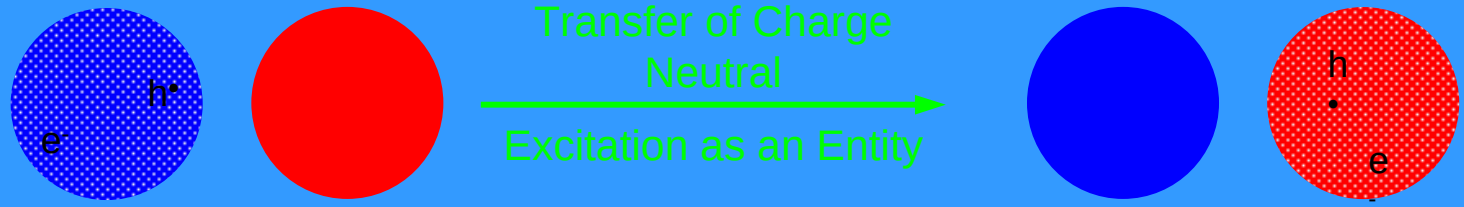

Excited Donor + Ground State Acceptor

$D^* + A$

Ground State Donor + Excited Acceptor

$D + A^*$

Radiationless Energy Transfer

$D^* + A \rightarrow D + A^*$

One Step Process

Near Field
d < 100 Å

Requires Coupling between the Excited Donor and Ground State Acceptor

Radiative Transfer

$D^* \rightarrow D + h\nu$

$A + h\nu \rightarrow A^*$

Two Step Process
"Real" Photon Mediates Energy Transfer

Far Field

No Direct Donor-Acceptor Interaction

Long Range Resonance Transfer of Excitations

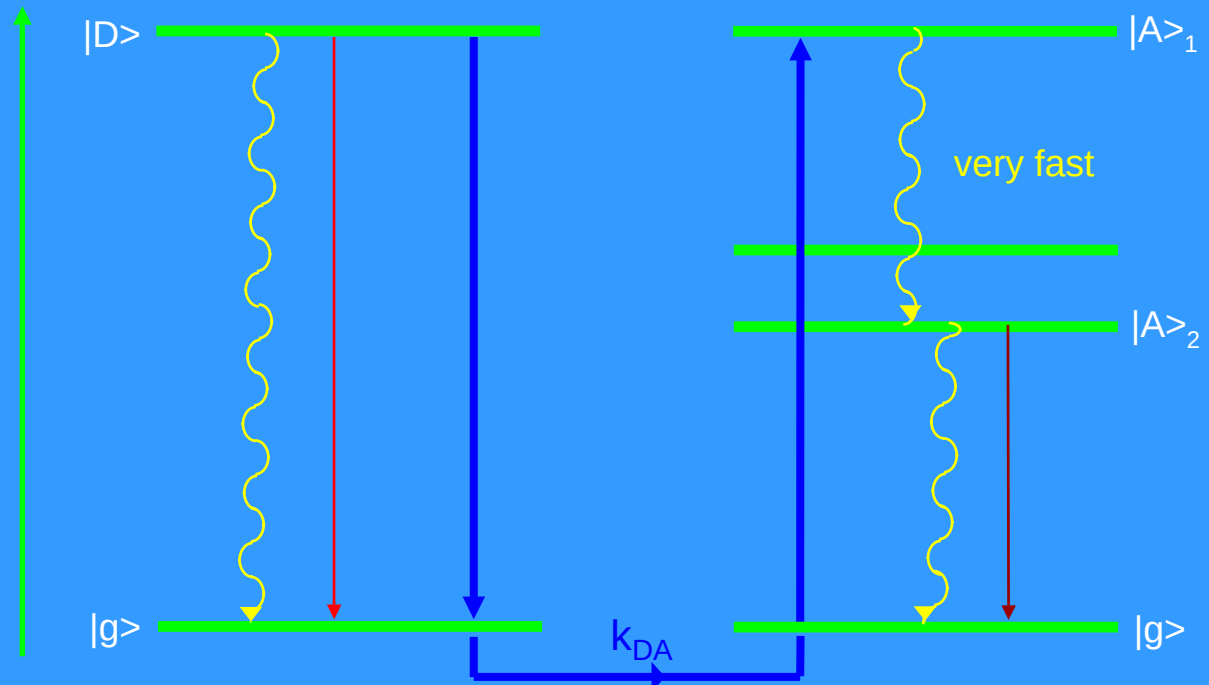

Couple via
Radiation Fields
Created by
Transition Dipoles

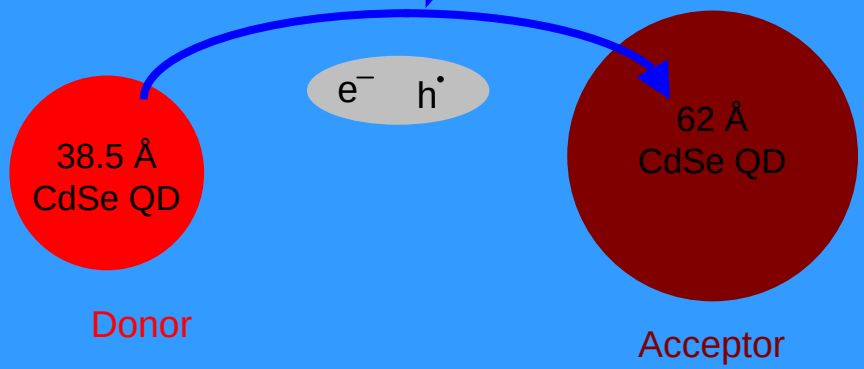

Quenching of Donor
Luminescence
Quantum Yield and Lifetime

Enhancement of Acceptor
Luminescence
Quantum Yield and Lifetime

Spectral Overlap of Donor Emission and Acceptor Absorption

Transition Dipole of Excited Donor → Normalized Spectrum for Donor Emission

Transition Dipole of Ground State Acceptor → Molar Extinction Coefficient for Acceptor Absorption

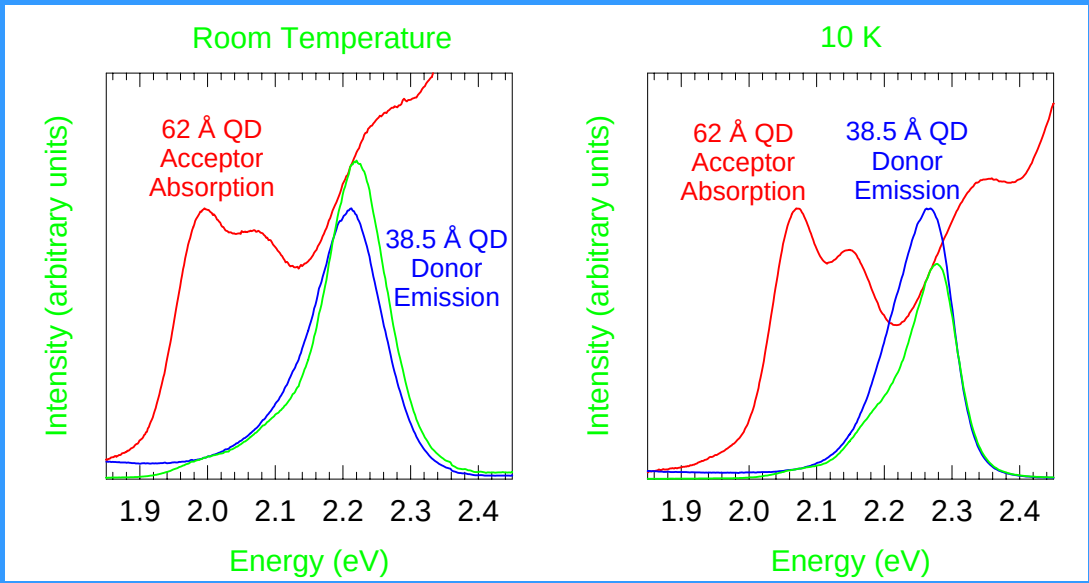

Spectral Overlap varies with Temperature as:
Spectral Features Shift Blue as T decreases
Narrow

Mixed CdSe Quantum Dot Solid

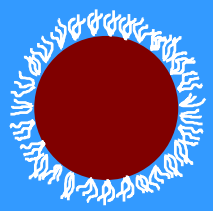

62 Å
CdSe QD

+

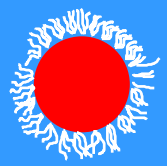

38.5 Å
CdSe QD

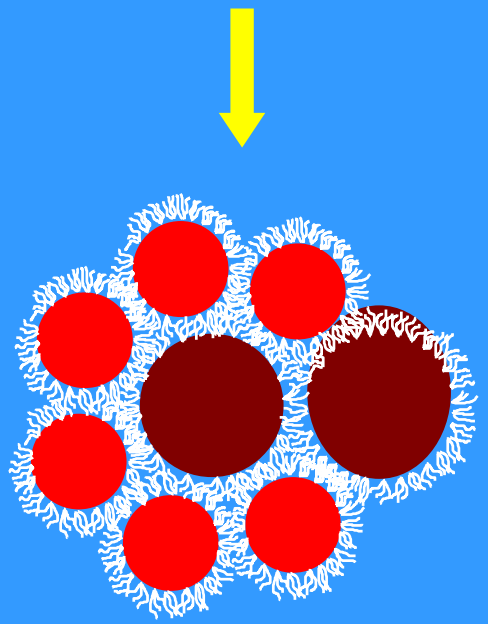

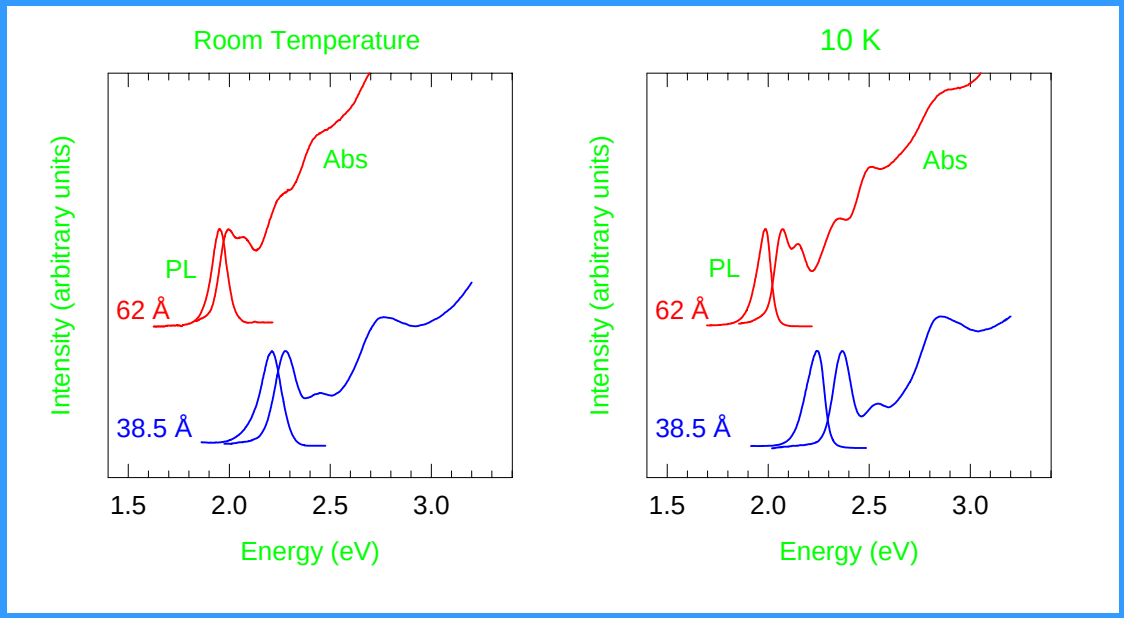

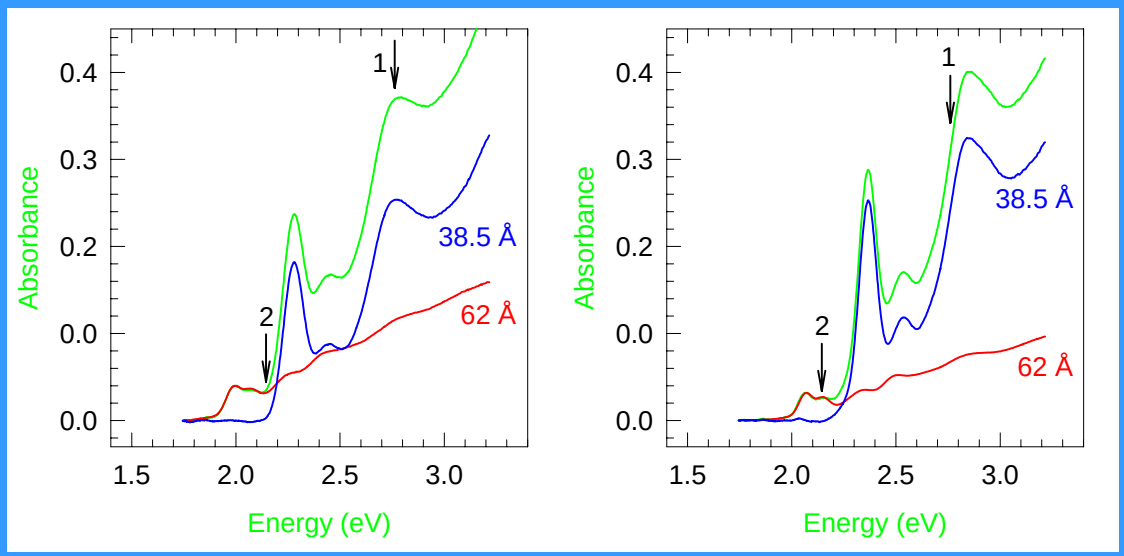

Efficiency of Long Range Resonance Transfer

$R_o \rightarrow$ "critical radius" -- distance of donor and acceptor separation at which

$$k_{D^* + A \rightarrow D + A^*} = \frac{1}{\tau_D}$$

Energy Transfer Rate

Donor Lifetime = Sum of Rates of De-excitation by other competing processes

Spectral Overlap of Donor Emission and Acceptor Absorption

Quantum Yield of Donor

$$R_o \propto \left(\frac{\varphi_D}{n^4} \int_0^\infty F_D(\tilde{\nu})\, \varepsilon_A(\tilde{\nu}) \frac{d\tilde{\nu}}{\tilde{\nu}^4} \right)^{1/6}$$

Index of Refraction

Spectral Overlap

R_o increases as φ_D increases by a factor of ~10 from RT to 10 K

$\Rightarrow$ 47 Å at Room Temperature

$\Rightarrow$ 67 Å at 10 K

compared to

$\Rightarrow R_{DA} = 61.25$ Å Nearest Neighbor Interaction

Room Temperature $k_{DA} = 1 \times 10^8$ sec^{-1}

Photoluminescence of a Mixed QD Solid and Solution Containing 82% 38.5 Å and 18% 62 Å CdSe Quantum Dots

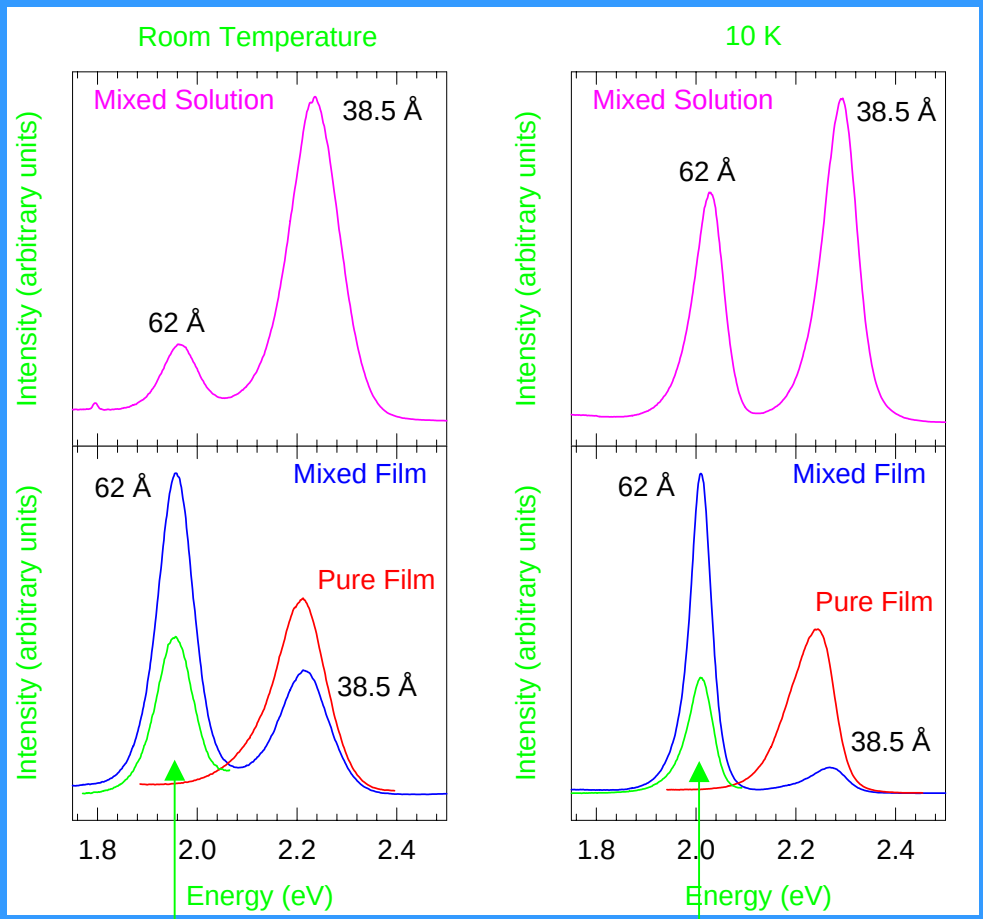

Mixed QD Solid Excited to the Red Of the 38.5 Å QDs Absorptions

Quenching of the Luminescence QY of the small 38.5 Å QDs accompanied by Enhancement of the Luminescence QY of the large 62 Å QDs in the Mixed CdSe QD Solid

C. R. Kagan, C. B. Murray, M. Nirmal, M. G. Bawendi, Phys. Rev. Lett. **76**, 1517 (1996).

Photoluminescence Excitation: The Origin of Emission

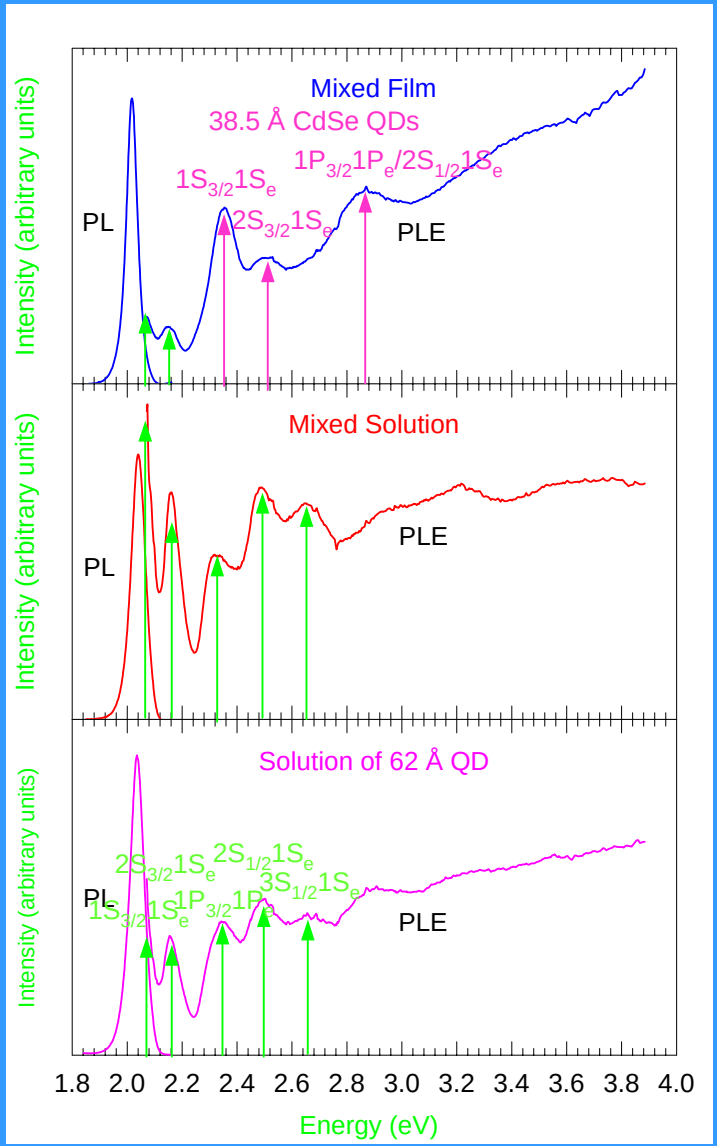

Time Dependence of Energy Transfer in Mixed QD Solids

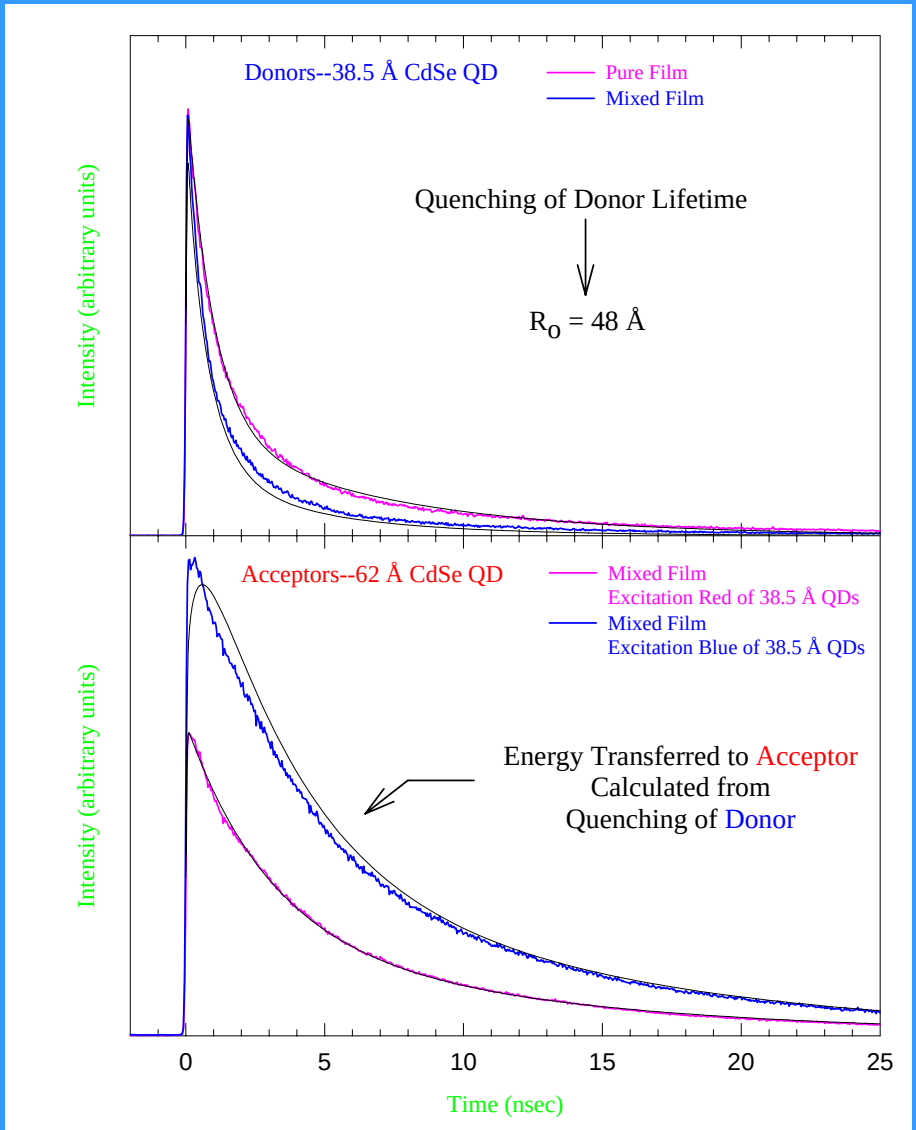

Energy Transfer within the Inhomogeneous Distribution of Electronic States

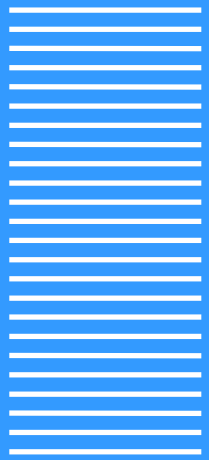

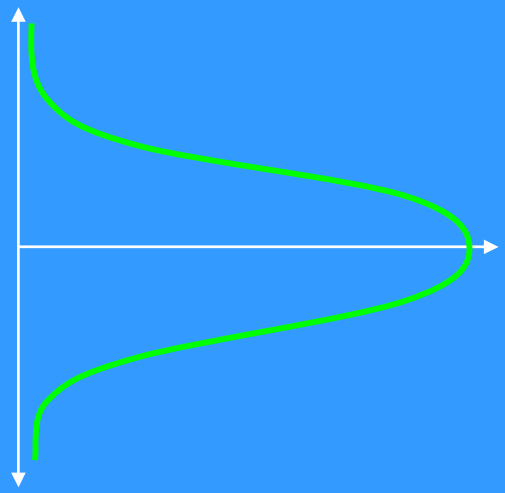

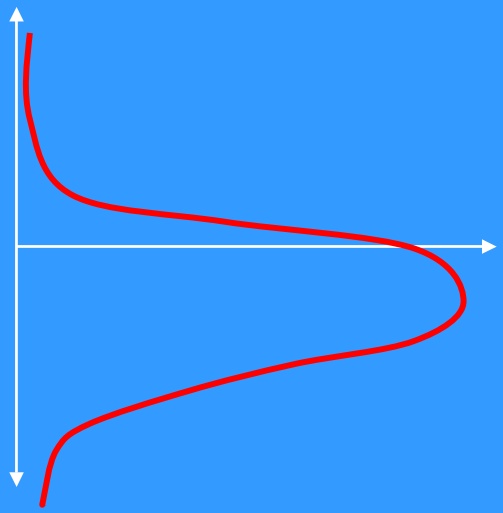

Inhomogeneous Distribution of Emission Energies in a QD Sample

Dispersed System

No Interaction between QDs

Close Packed System

Energy Transfer between Proximal QDs

QDs Dispersed in Solution → Close Packed in QD Solid

→ Red Shift
→ Narrowingof the Emission Lineshape
→ Asymmetric

C. R. Kagan, C. B. Murray, M. G. Bawendi, Phys. Rev. B **54**, 8633 (1996).

Energy Transfer within the Sample Inhomogeneous Distribution

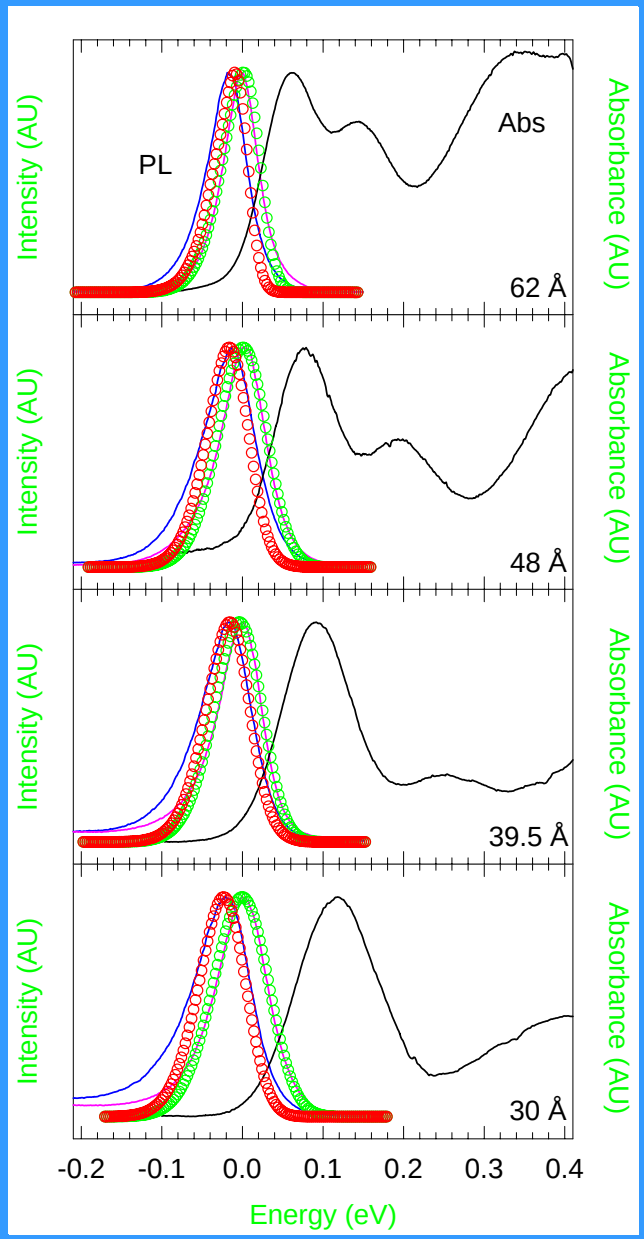

Experimental
Solution Luminescence

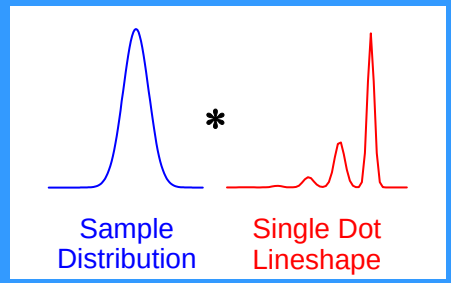

Fit Solution
Luminescence

↓

Sample
Distribution

Energy Transfer
within
Sample
Distribution

↓

Efficiency
Calculated
From
Spectral Overlap

Calculated
Film Luminescence

reproduces

Experimental
Film Luminescence

Probability of Energy Transfer

$$P_{DA} = \frac{R_o^6}{R_o^6 + R_{DA}^6}$$

Spectral Overlap from the Absorption Spectrum for the QD Solid, Emission Spectrum for the QDs in Solution, Quantum Yield of the QD Solid

Nearest Neighbor Distance in QD Solid

D	R_o	R_{DA}	P_{DA}
30 Å	37.9 Å	41.3 Å	0.38
39.5 Å	35.4 Å	50.4 Å	0.11
48 Å	47.3 Å	59.1 Å	0.21
62 Å	53.9 Å	73.1 Å	0.14

R_o and P_{DA} vary with the Quantum Yield for the QD Solid

R_o increases

↓

Spectral Overlap increases

↓

Stokes shift between Absorption and Emission Spectra decreases

P_{DA} decreases

↓

R_{DA} increases faster than R_o

Broad versus Narrow Size Distribution

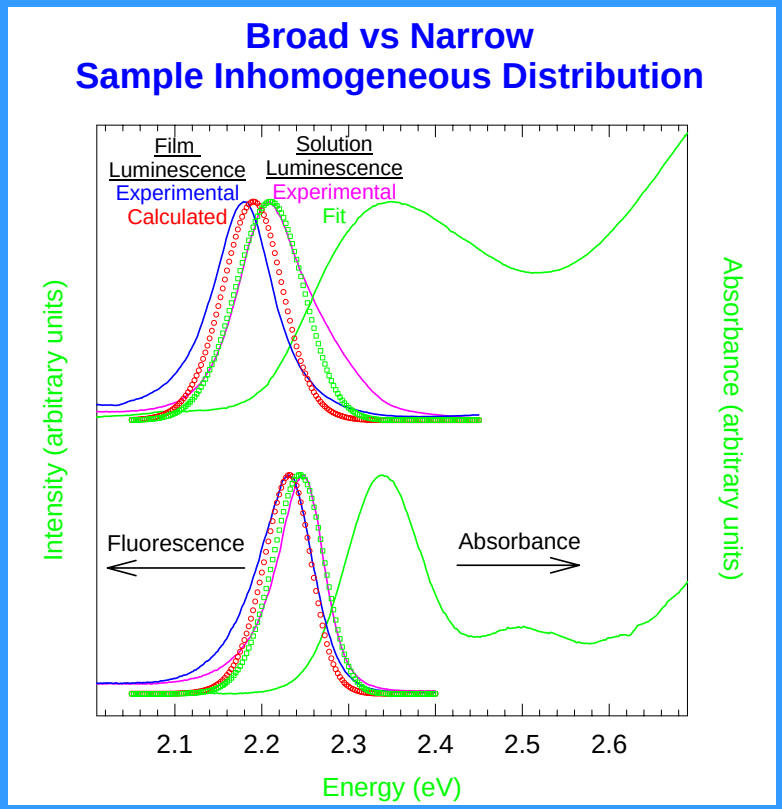

Peak in Emssion Shifts Red

Narrow Distribution $\Delta E = 14.6$ meV
Broad Distribution $\Delta E = 29.6$ meV

Emission Lineshape Narrows

Narrow Distribution $\Delta FWHM = 11$ meV
Broad Distribution $\Delta FWHM = 23$ meV

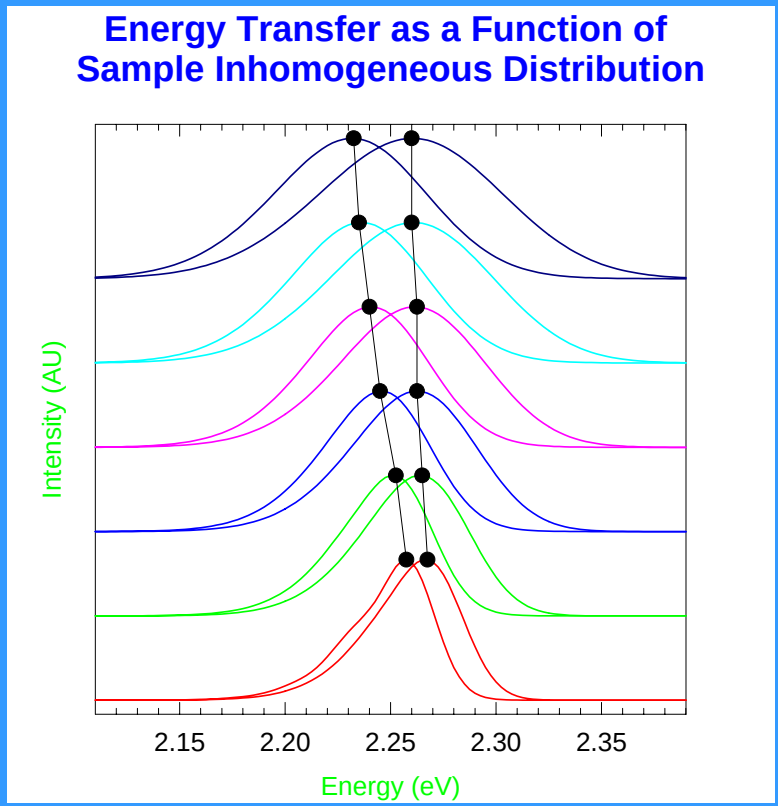

Red Shift Increases
with Increasing
Sample Inhomogeneous Distribution

Emission Lineshape Narrows
from Solution → Film

Narrowning Increases
with Increasing
Sample Inhomogeneous Distribution

Concentration Dependence of Luminscence Lineshape

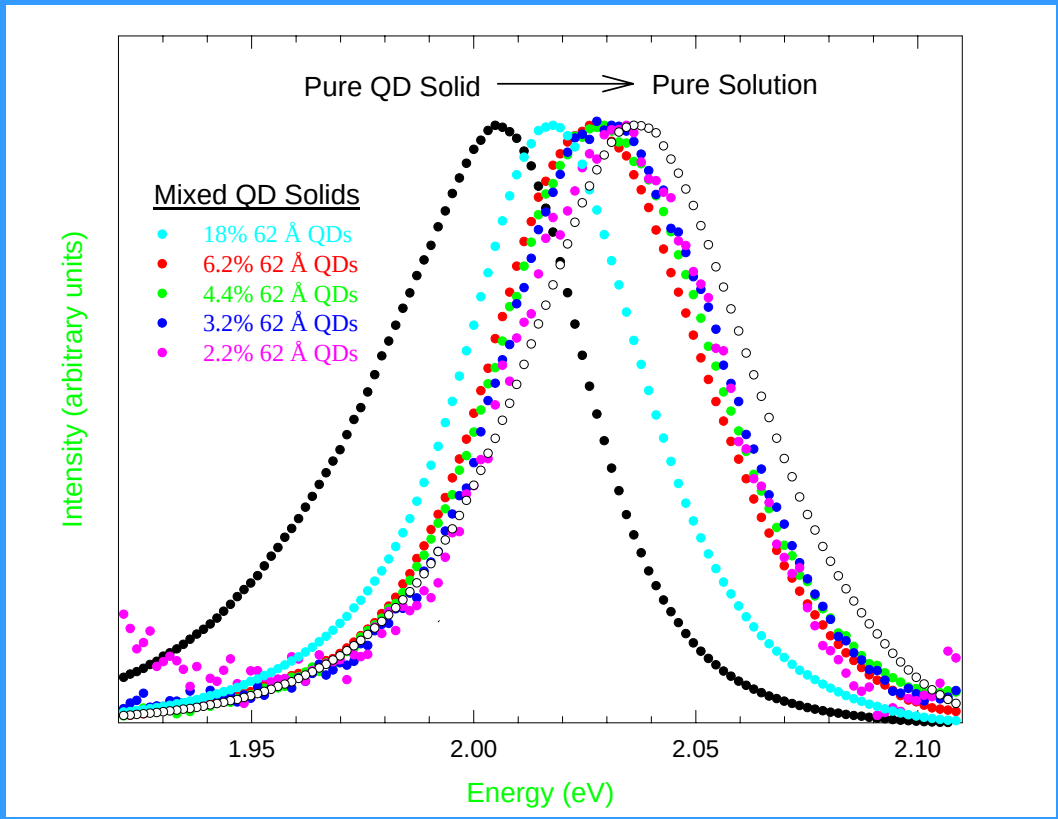

Luminescence Lineshape { Shift Blue → Solution; Asymmetric → "Gaussian-like" } as

Decreasing Concentration of 62 Å QDs in Matrix of 38.5 Å QDs

⬇

Increases Average Separation between 62 Å QDs

⬇

Reduces Probability of Energy Transfer between 62 Å QDs

AFC media magnetization response to magnetic field

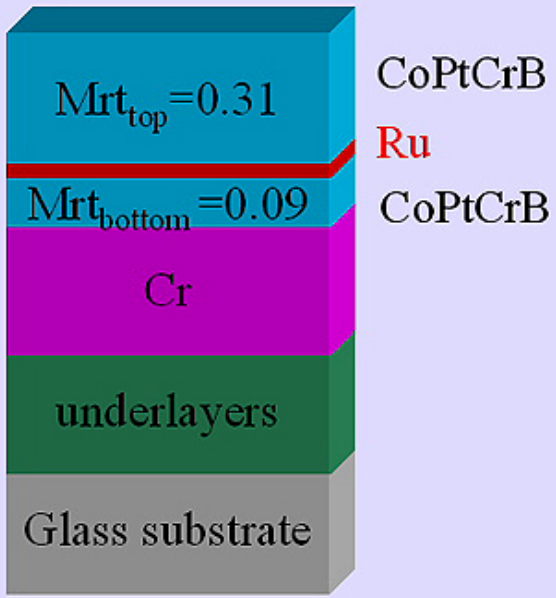

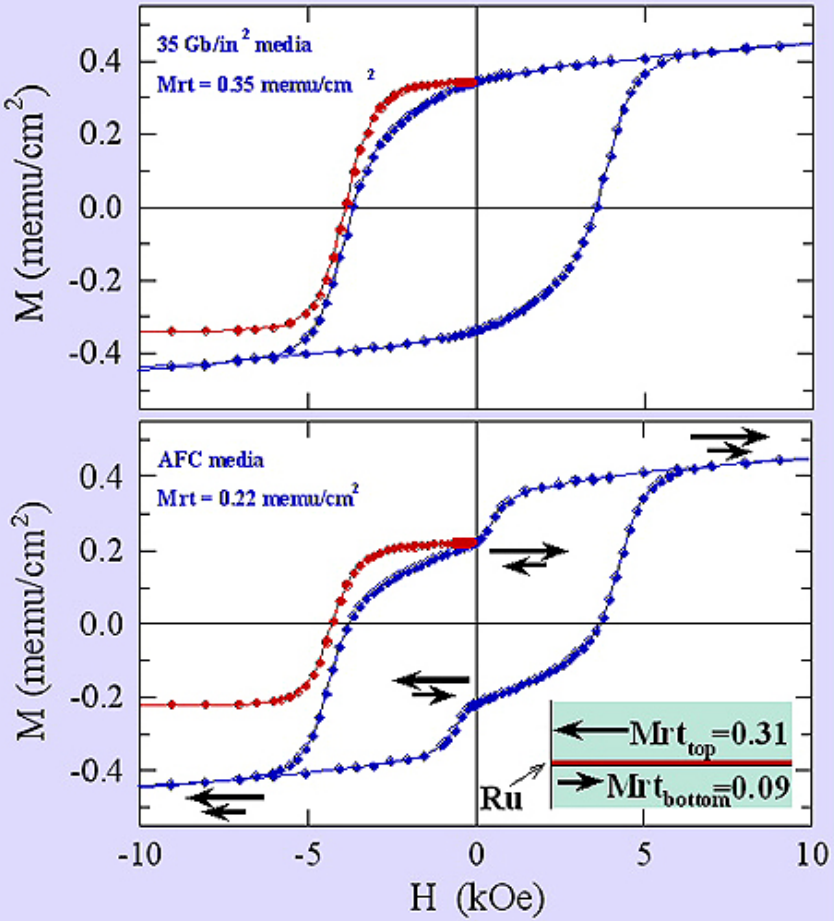

IBM

Fullerton, E. et. al., Appl. Phys. Lett., 77, 3806, 2000

Exchange-Spring Nanocomposites via Self-Assembly

A super strong magnet will enable





material requirements: High M_s, high H_c, high $(BH)_{max}$

nature limits: M_s vs. H_c

solution: exchange-spring magnets

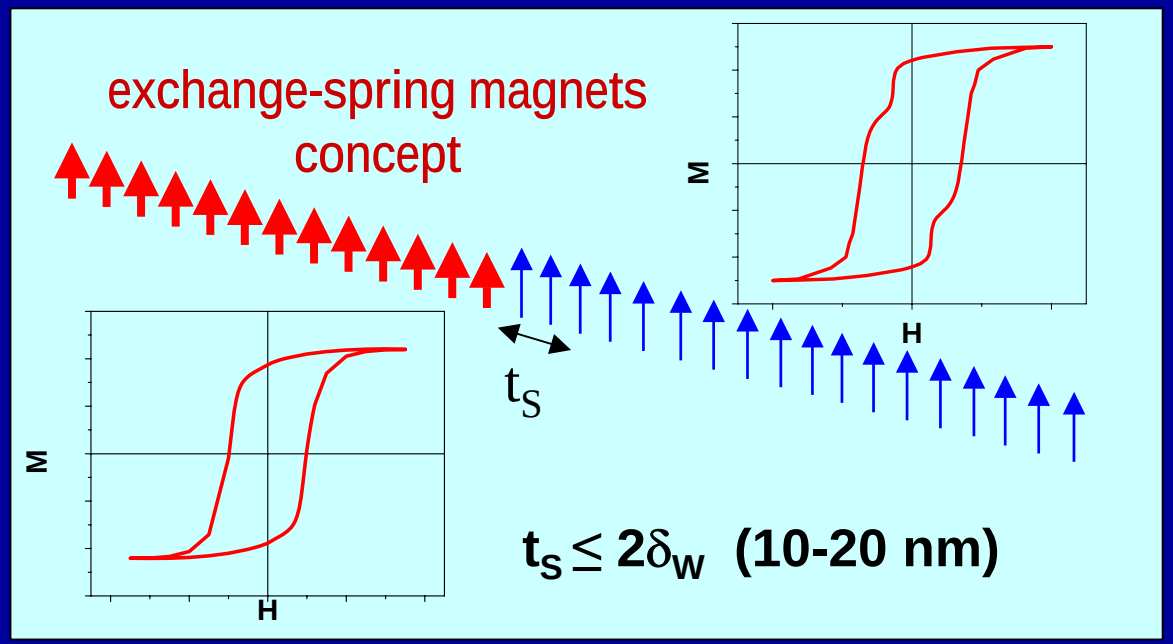

nanoparticle self-assembly-bottom-up approach

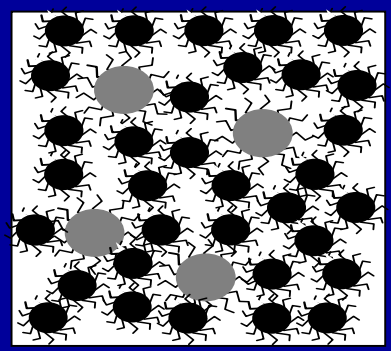
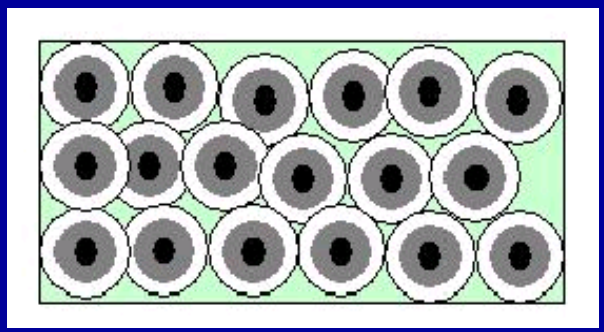

Nanoscale Engineering for Optimum Exchange-Coupling

Nature, 420, 395 (2002)

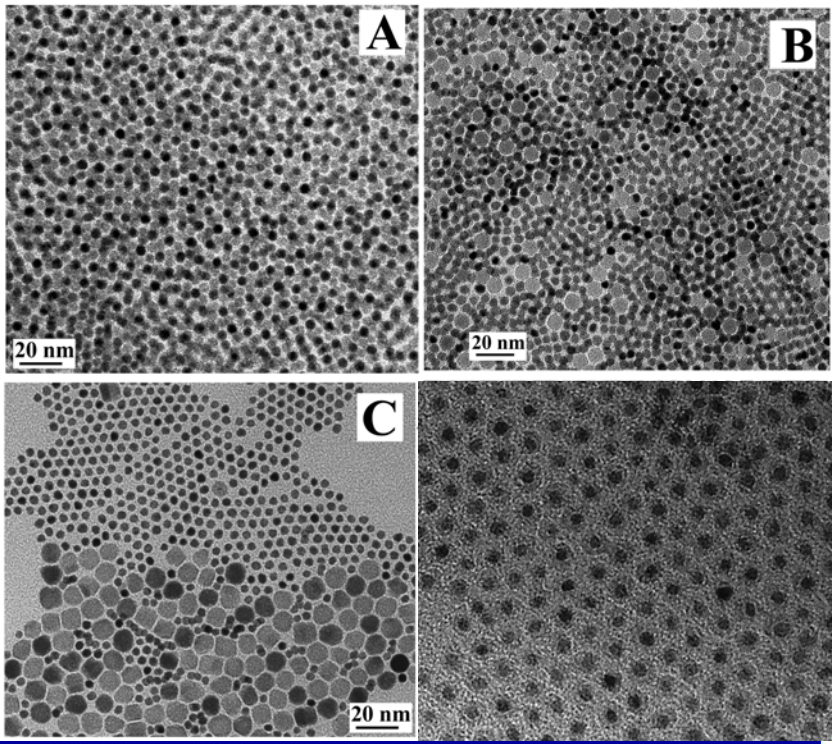

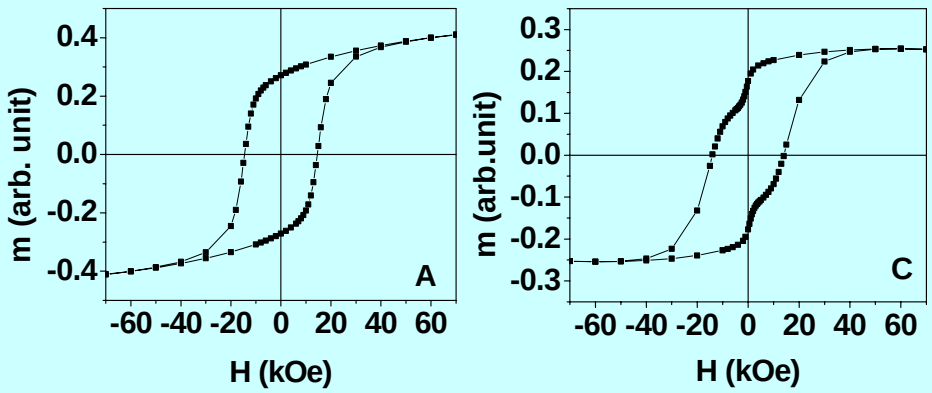

Hysteresis loops of FePt-Fe_3Pt nanocomposite derived from Fe_3O_4:FePt binary assembly (A) 4 nm:4 nm; and (C) 12 nm:4 nm

TEM images of the binary composite assemblies of

(A) Fe_3O_4(4 nm):$Fe_{58}Pt_{42}$(4 nm);
(B) Fe_3O_4(8 nm):$Fe_{58}Pt_{42}$(4 nm);
(C) Fe_3O_4(12 nm):$Fe_{58}Pt_{42}$(4 nm);
(D) FePt)Fe_3O_4 core-shell

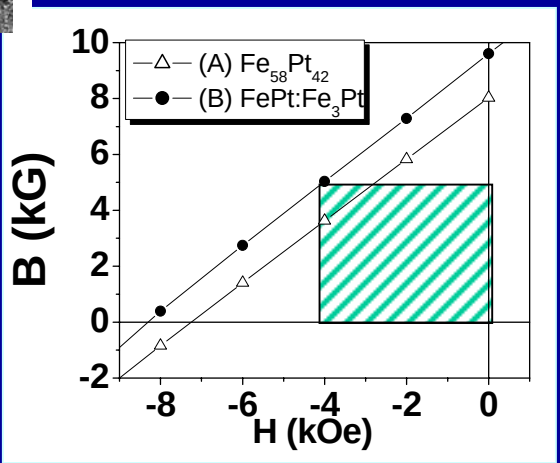

36% energy product enhancement compared to single-phase FePt!

Binary nanocomposites

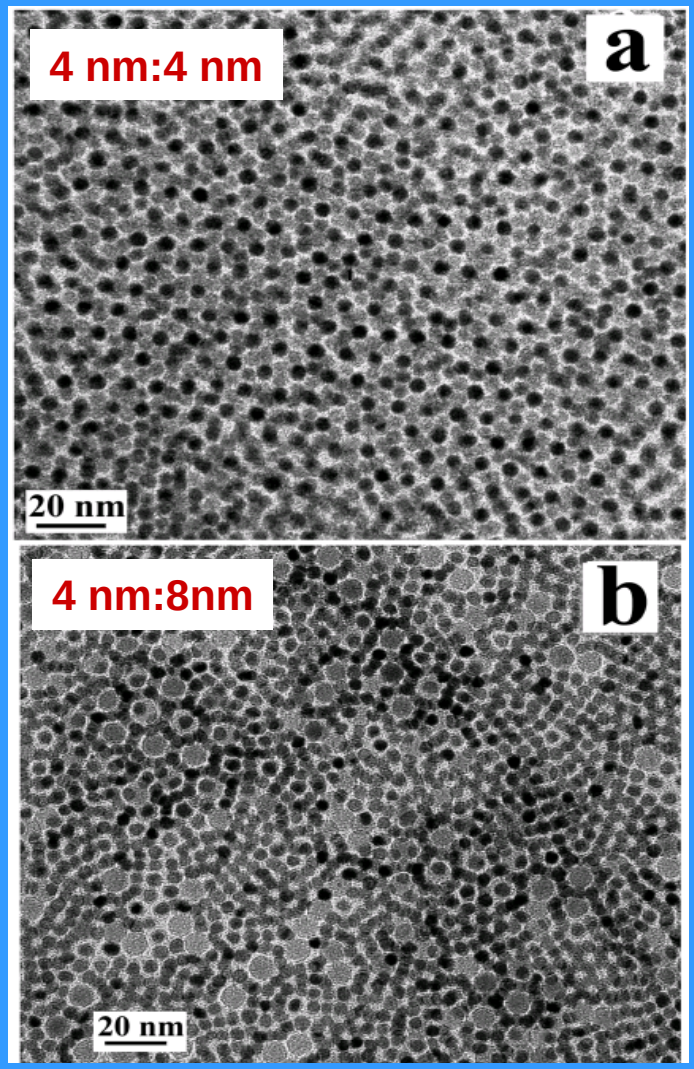

TEM images of two different binary assemblies prepared directly from particle dispersions of 4 nm FePt as well as 4 nm Fe_3O_4 and 8 nm Fe_3O_4.

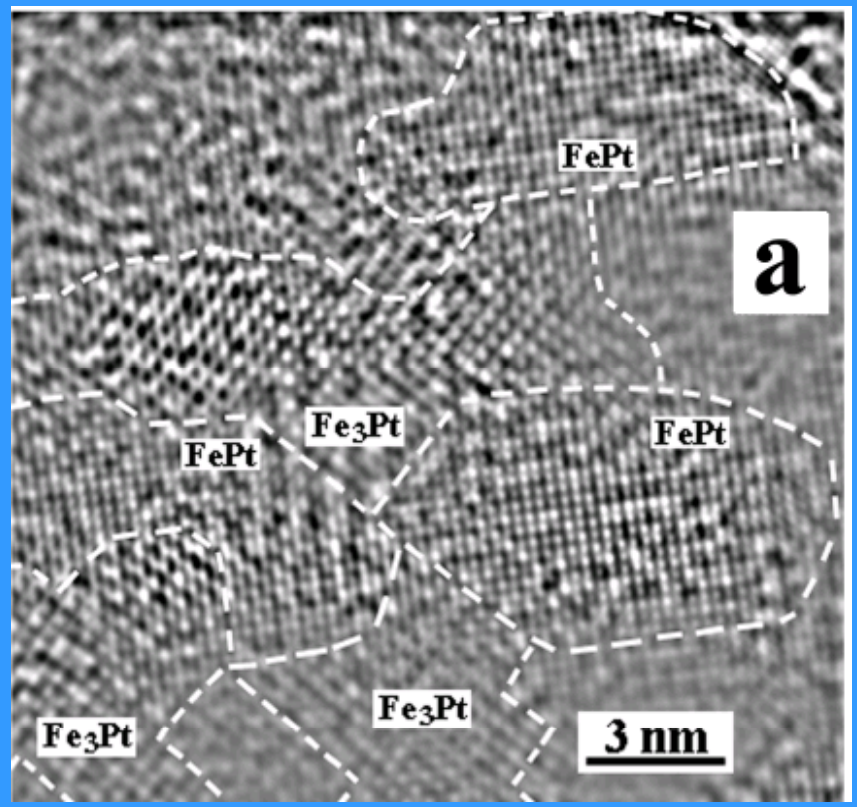

HRTEM image of an exchange-coupled nanocomposite (FePt-Fe_3Pt) made from 4nm FePt and 4nm Fe_3O_4 nanoparticles under reductive annealing. Shown here is a modulated structure with FePt and Fe_3Pt in intimate contact, resulting in exchange-coupling.

H. Zeng et al, *Nature*, **2002**, *420*, 395.

Nanocomposite magnetics

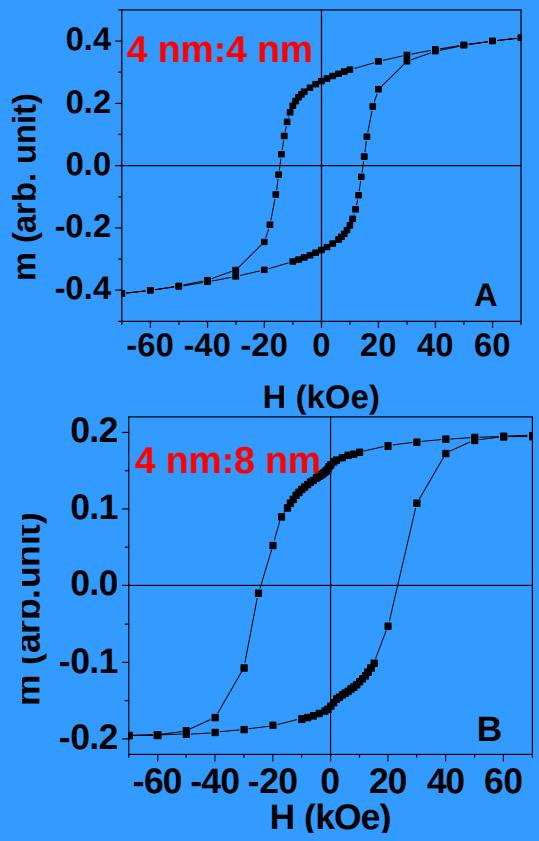

Hysteresis loops at room temperature with the composites from 4nm:4nm and 4nm:8nm nanoparticles respectively.

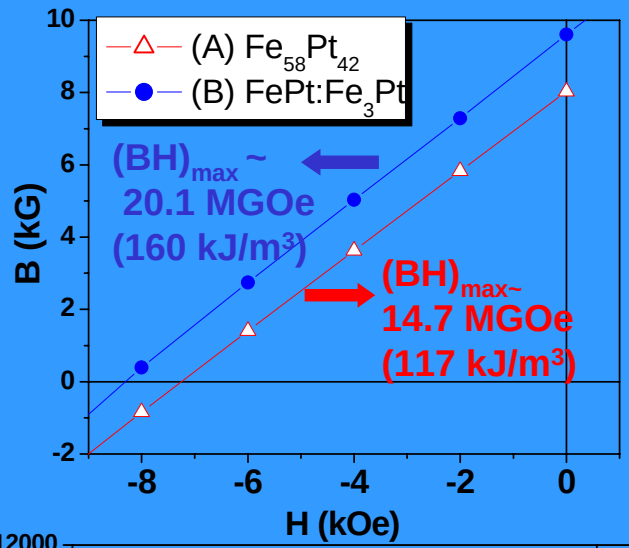

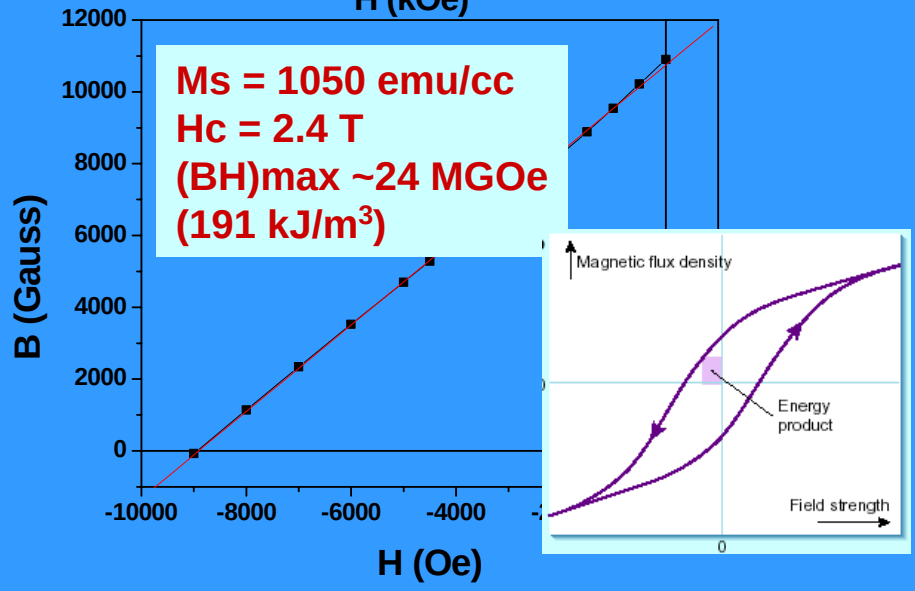

(BH)max, energy product, reflects the ability for a composite to store the magnetic energy, the larger the better.

Binary Nanocrystal Array's a New Class of Nanostructured Materials

Franz Redl, Kyung-Sang Cho and C. B. Murray

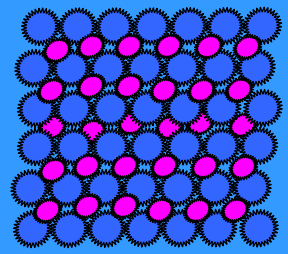

Binary Assembly

AB_{13}

Composites of:Ferromagnets, Noble Metals, Semiconductor QDs, Ferroelectrics, Superconductors, may all be possible.

New Near IR Magneto-Optic Composite ~13nm Fe2O3 and 5nm PbSe QDots

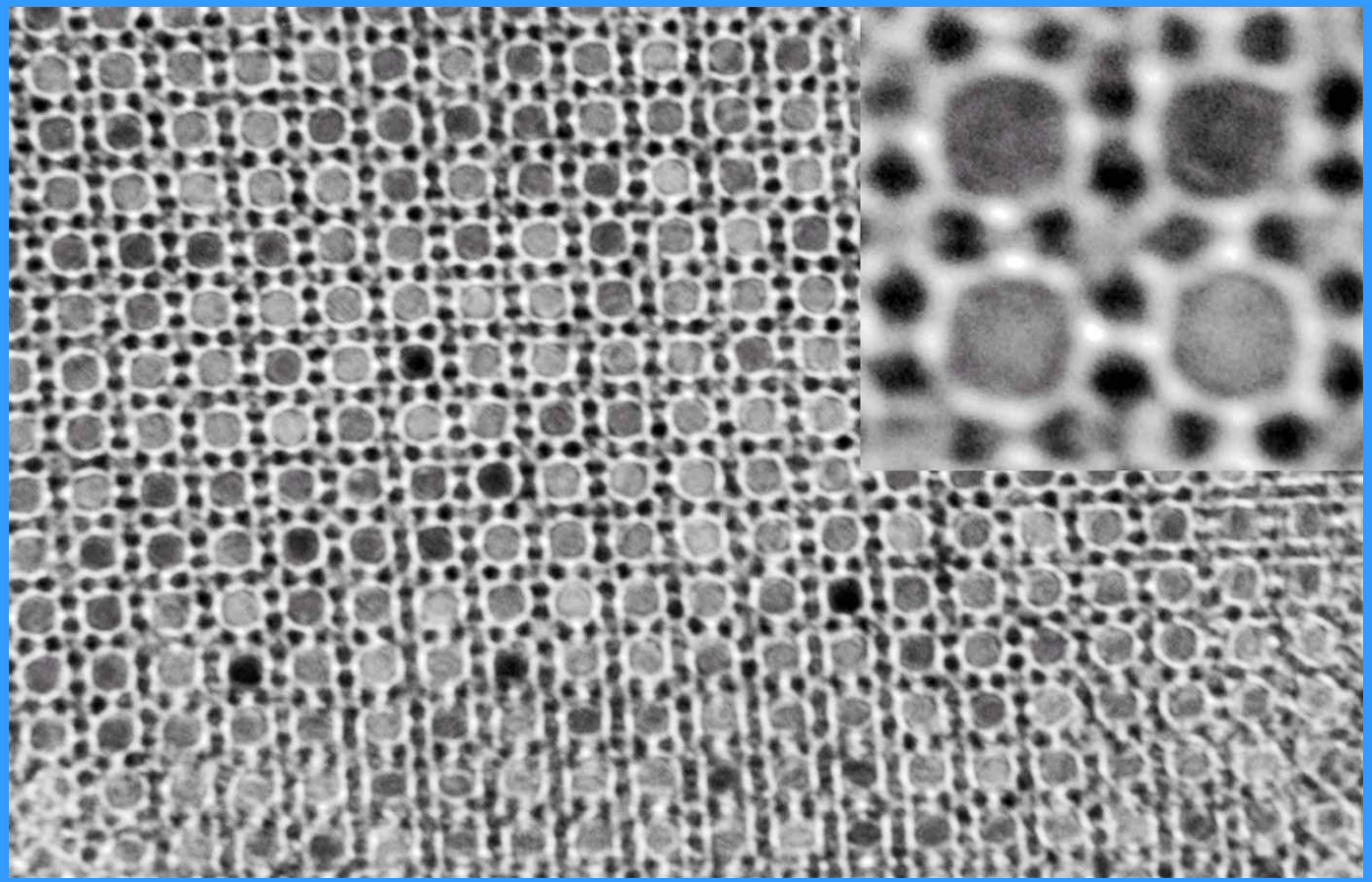

Binary nanocomposites *via* self-assembly of two kinds of NPs

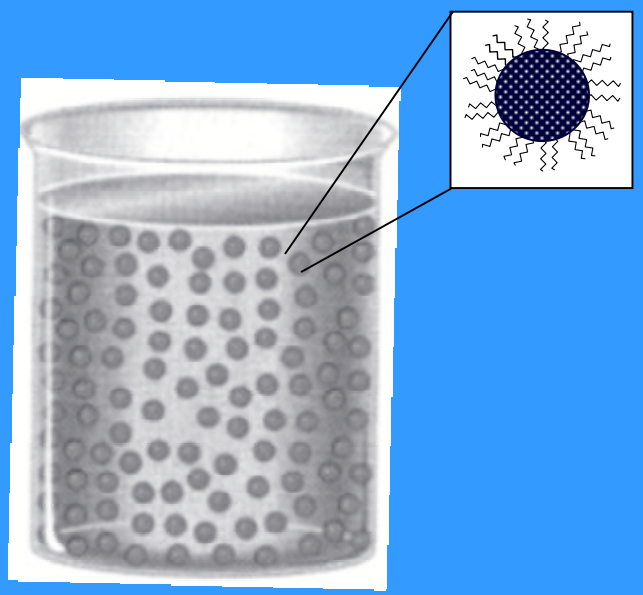

A nanoparticle dispersion in an organic solvent. The particles are stabilized by a layer of organic surfactant to prevent them from aggregation.

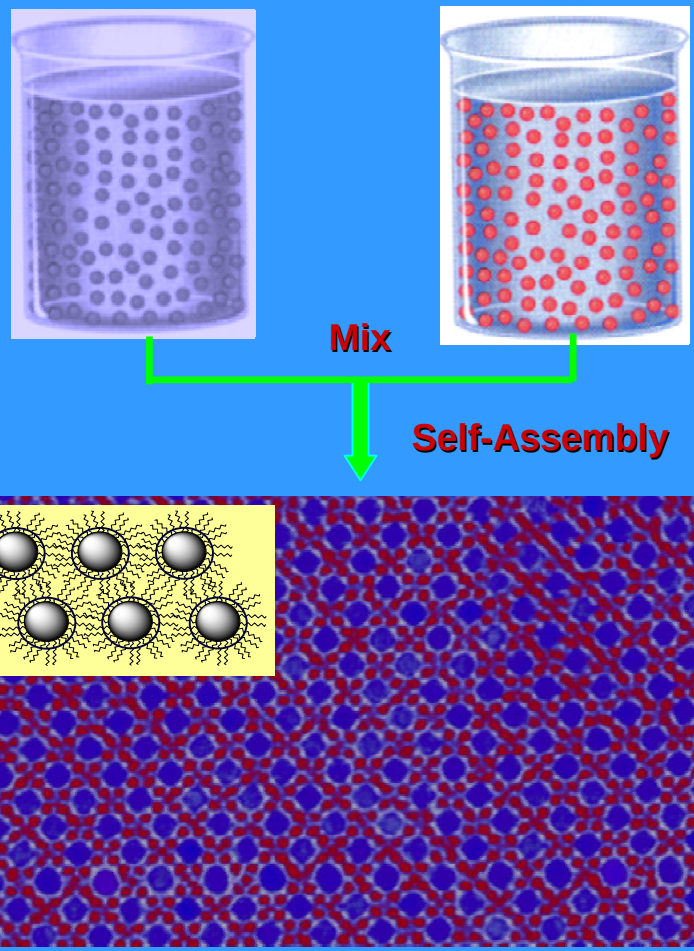

Binary nanocomposite: Magnetic-magnetic composite or magnetic-semiconductor composite.

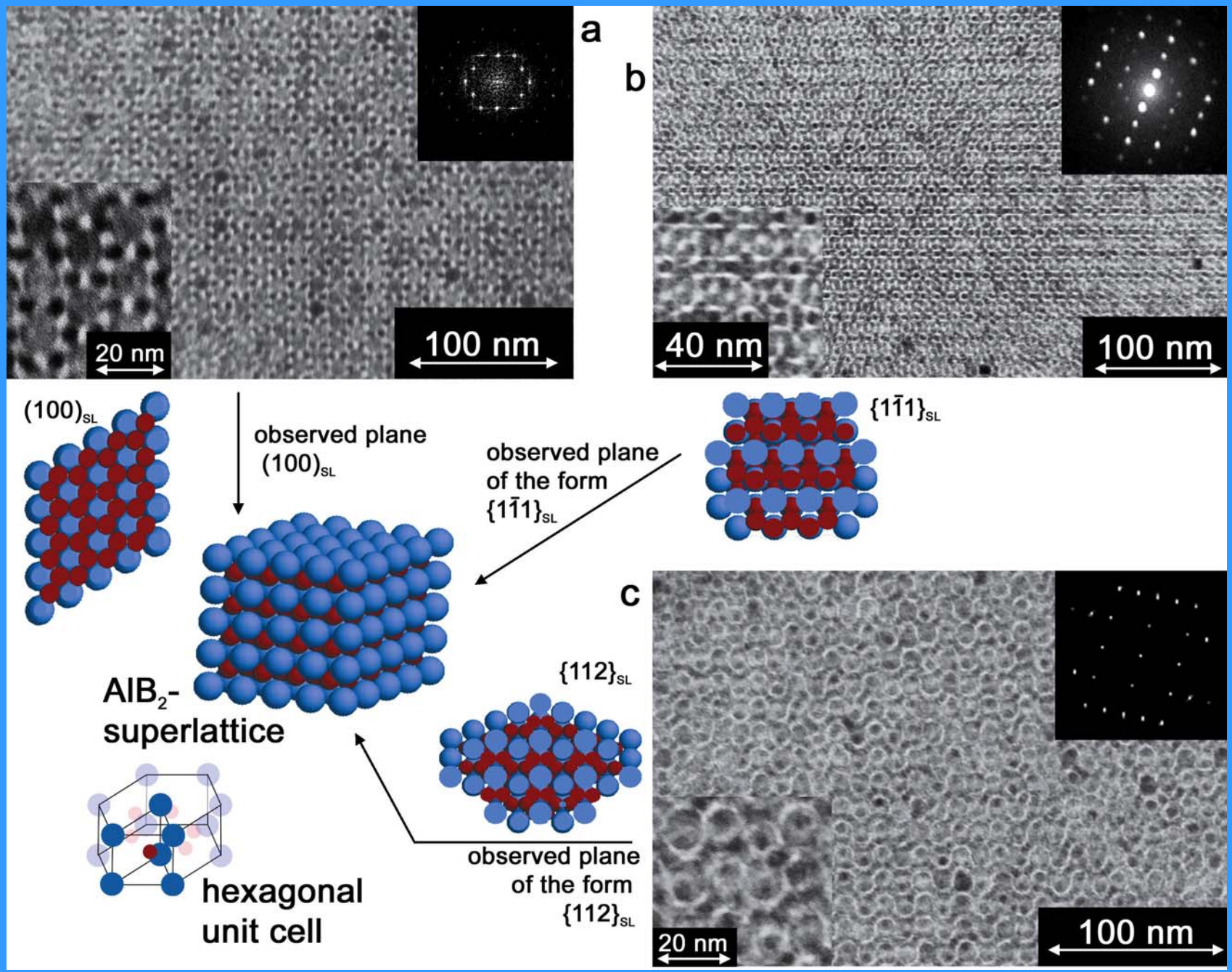
a
b
20 nm
100 nm
40 nm
100 nm
$(100)_{SL}$
observed plane
$(100)_{SL}$
observed plane
of the form
$\{1\bar{1}1\}_{SL}$
$\{1\bar{1}1\}_{SL}$
c
AlB_2-
superlattice
$\{112\}_{SL}$
observed plane
of the form
$\{112\}_{SL}$
hexagonal
unit cell
20 nm
100 nm

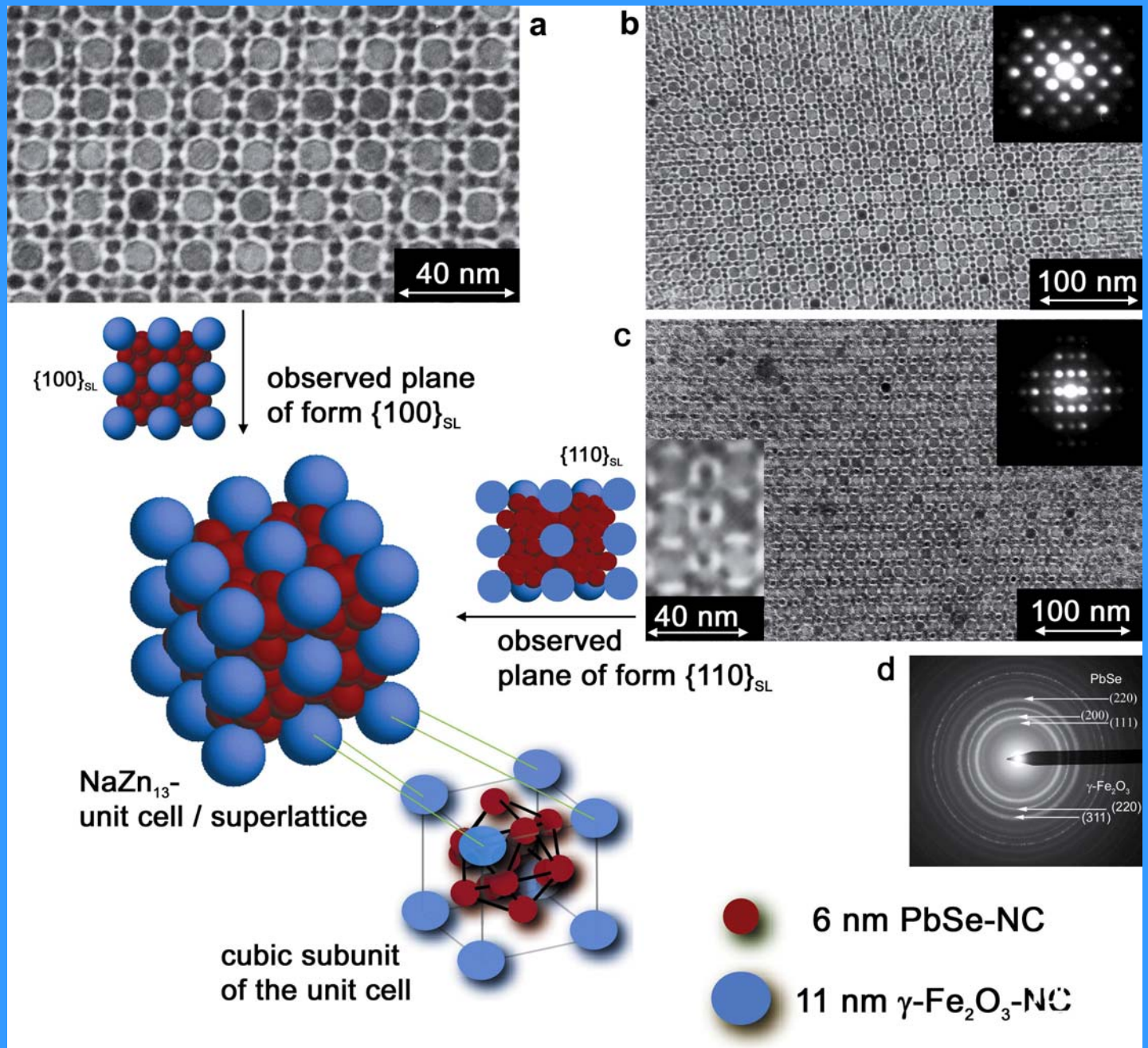
a
b
40 nm
100 nm
{100}SL
observed plane
of form {100}SL
c
{110}SL
40 nm
100 nm
observed
plane of form {110}SL
d
PbSe
(220)
(200)
(111)
γ-Fe2O3
(220)
(311)
NaZn13-
unit cell / superlattice
cubic subunit
of the unit cell
6 nm PbSe-NC
11 nm γ-Fe2O3-NC

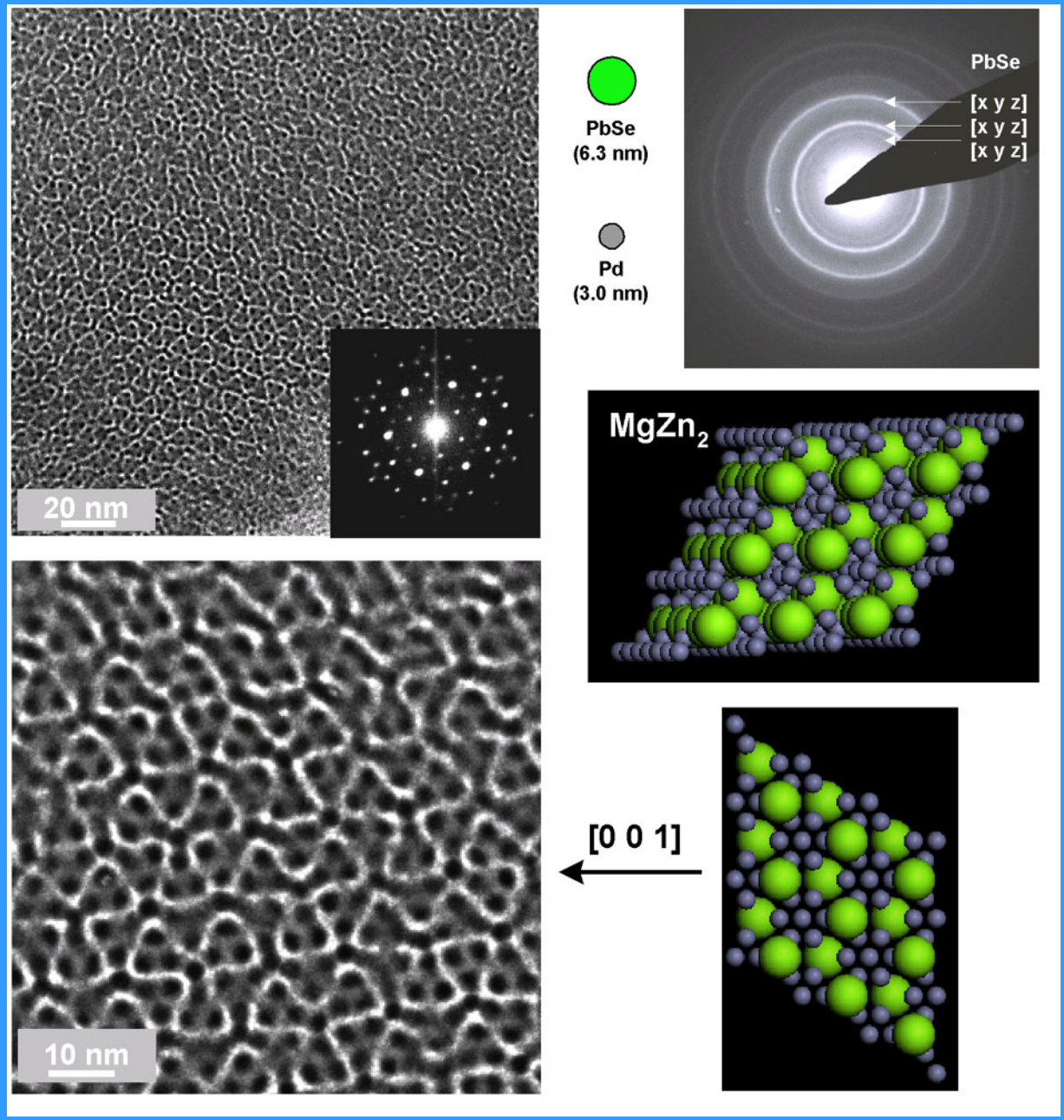
20 nm
PbSe
(6.3 nm)
Pd
(3.0 nm)
PbSe
[x y z]
[x y z]
[x y z]
MgZn2
10 nm
[0 0 1]

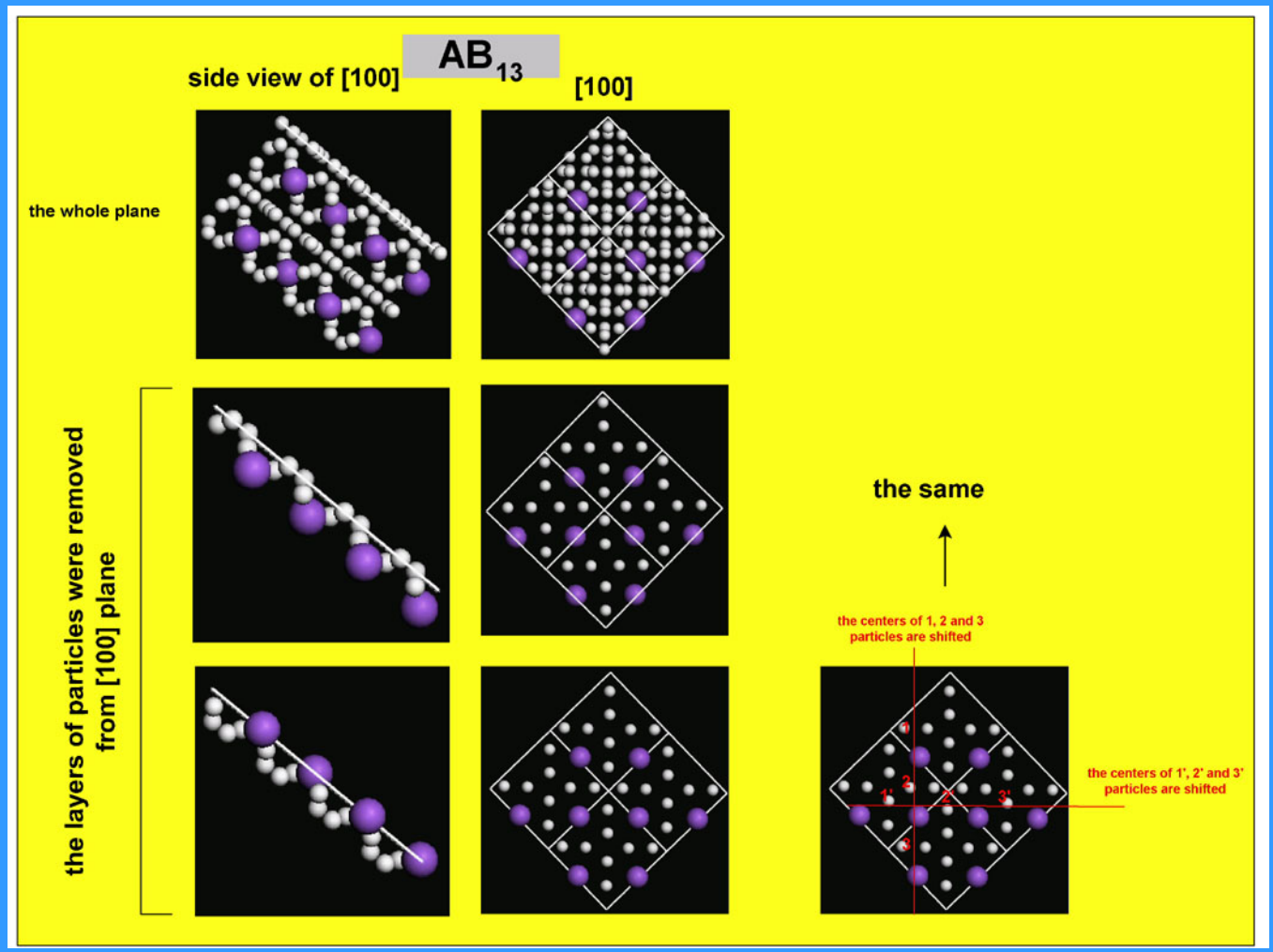
AB13
side view of [100]
[100]
the whole plane
the layers of particles were removed from [100] plane
the same
the centers of 1, 2 and 3 particles are shifted
the centers of 1', 2' and 3' particles are shifted
1
2
3
1'
2'
3'

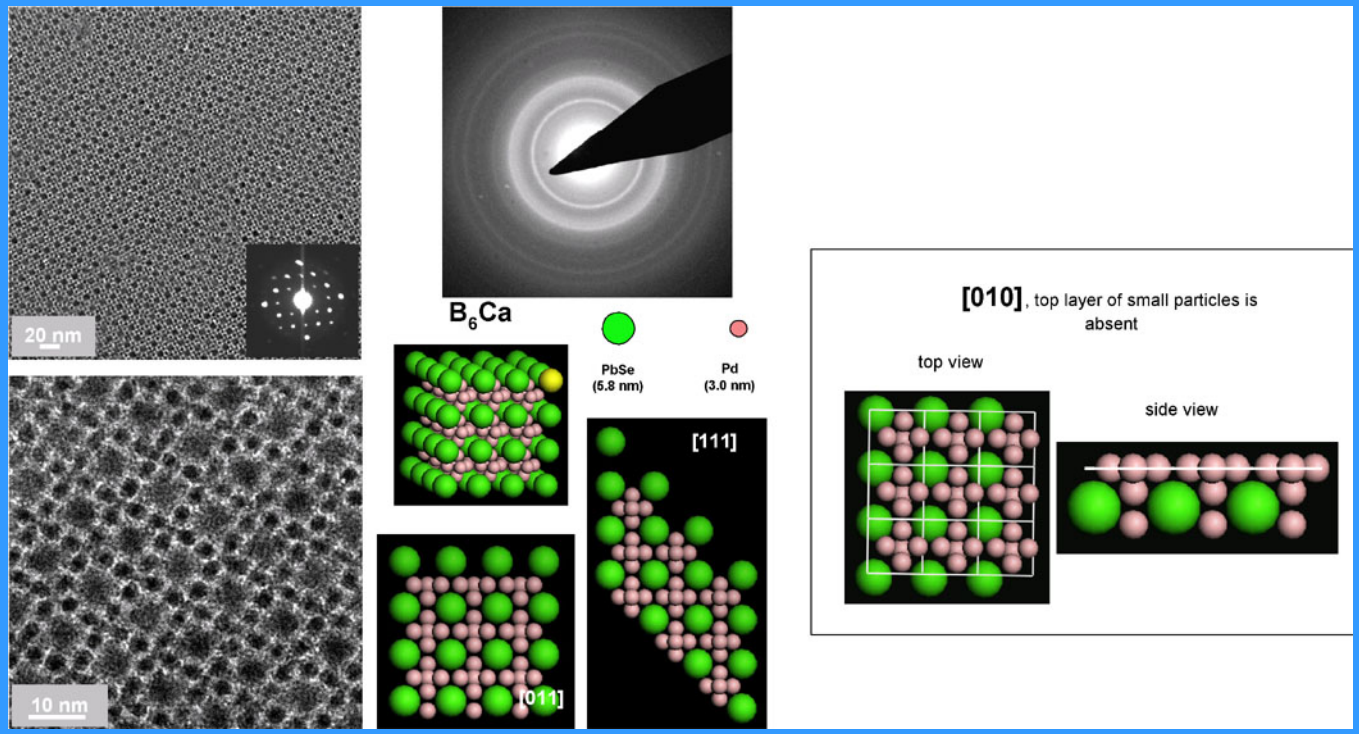
20 nm
10 nm
B6Ca
PbSe
(5.8 nm)
Pd
(3.0 nm)
[111]
[011]
[010], top layer of small particles is absent
top view
side view

PbSe – Au binary mixture

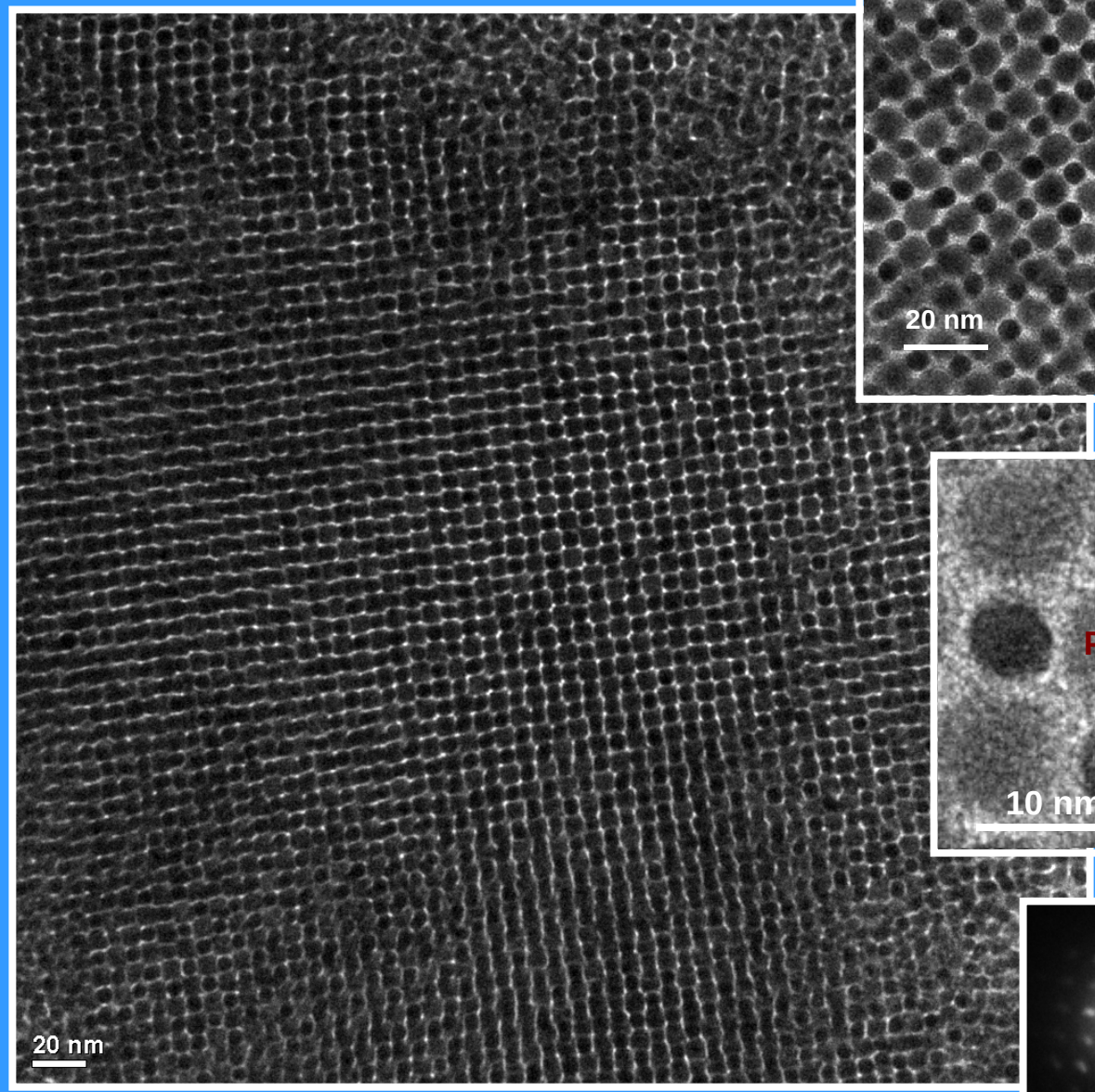

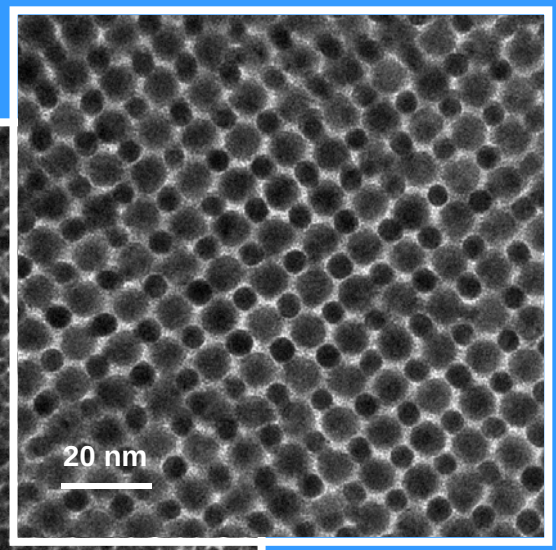

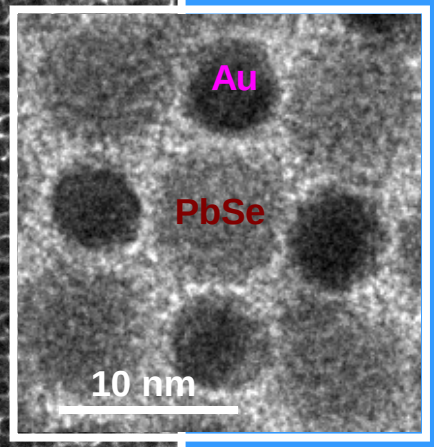

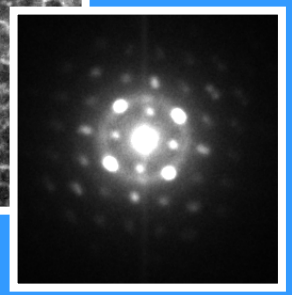

Fe_2O_3 – Au binary mixture

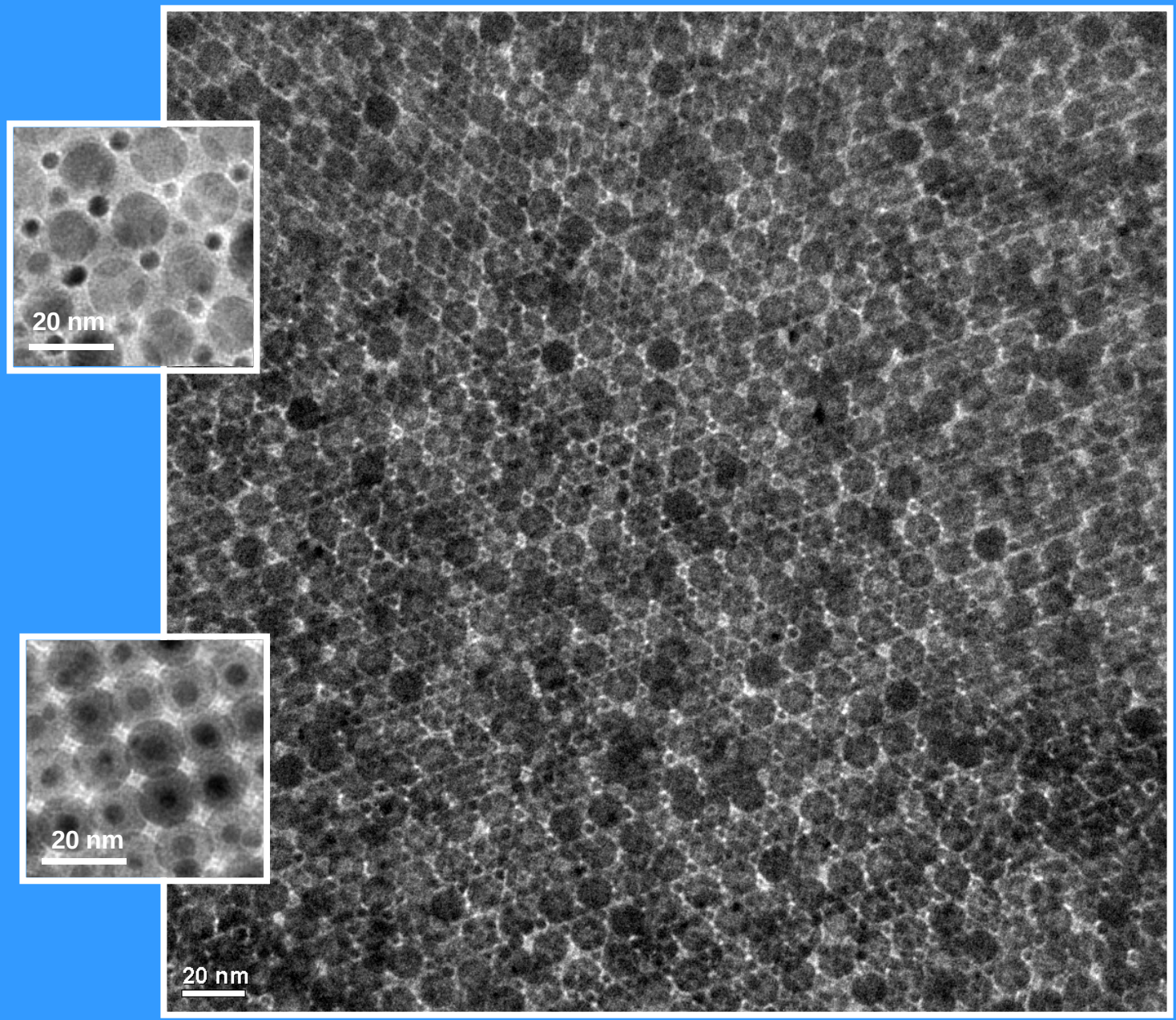

PbSe – Ag binary nanoparticle mixture

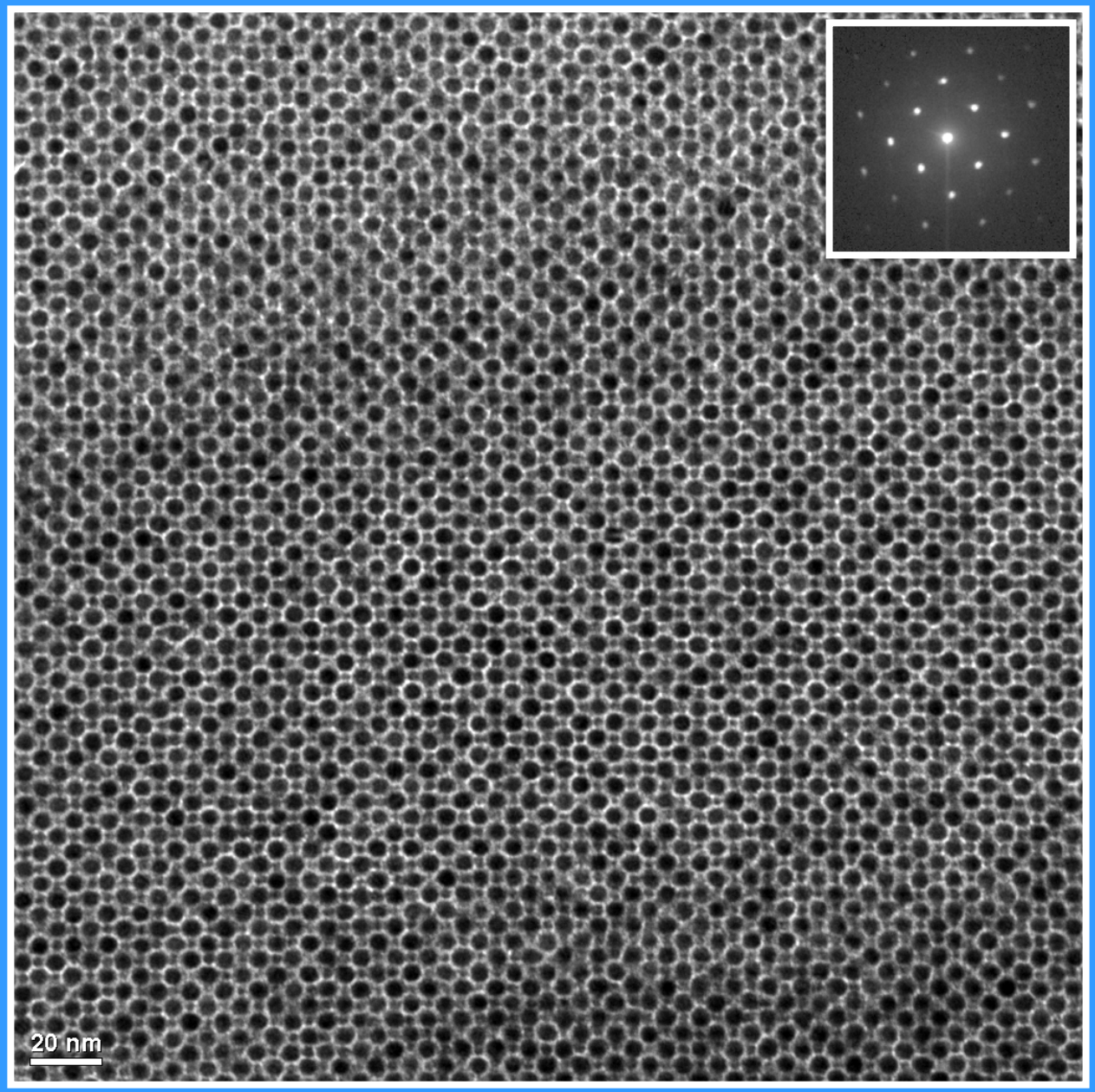

PbSe (large) – Ag (small) binary nanoparticle mixture

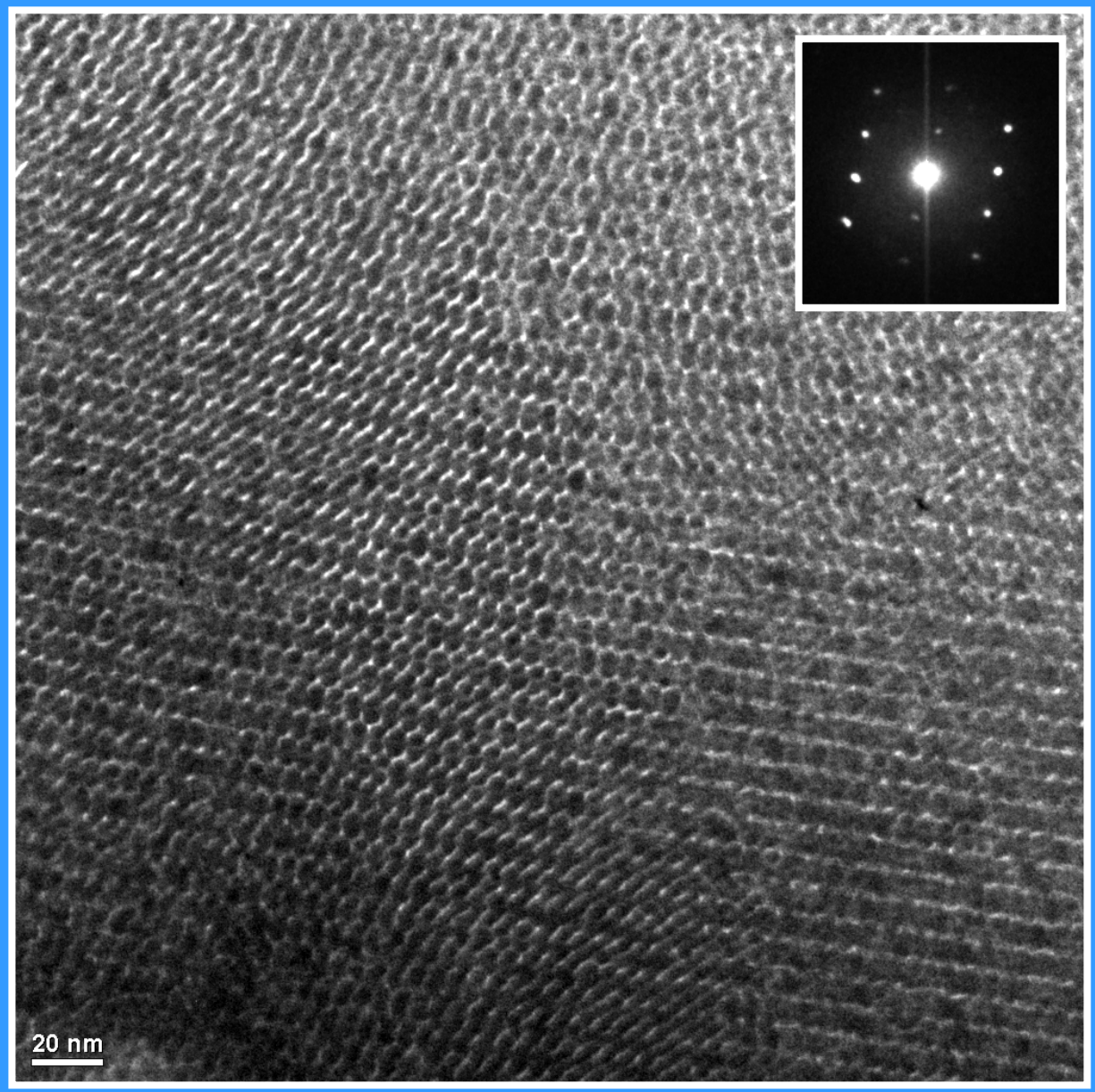

PbSe (large) – Ag (small) binary nanoparticle mixture

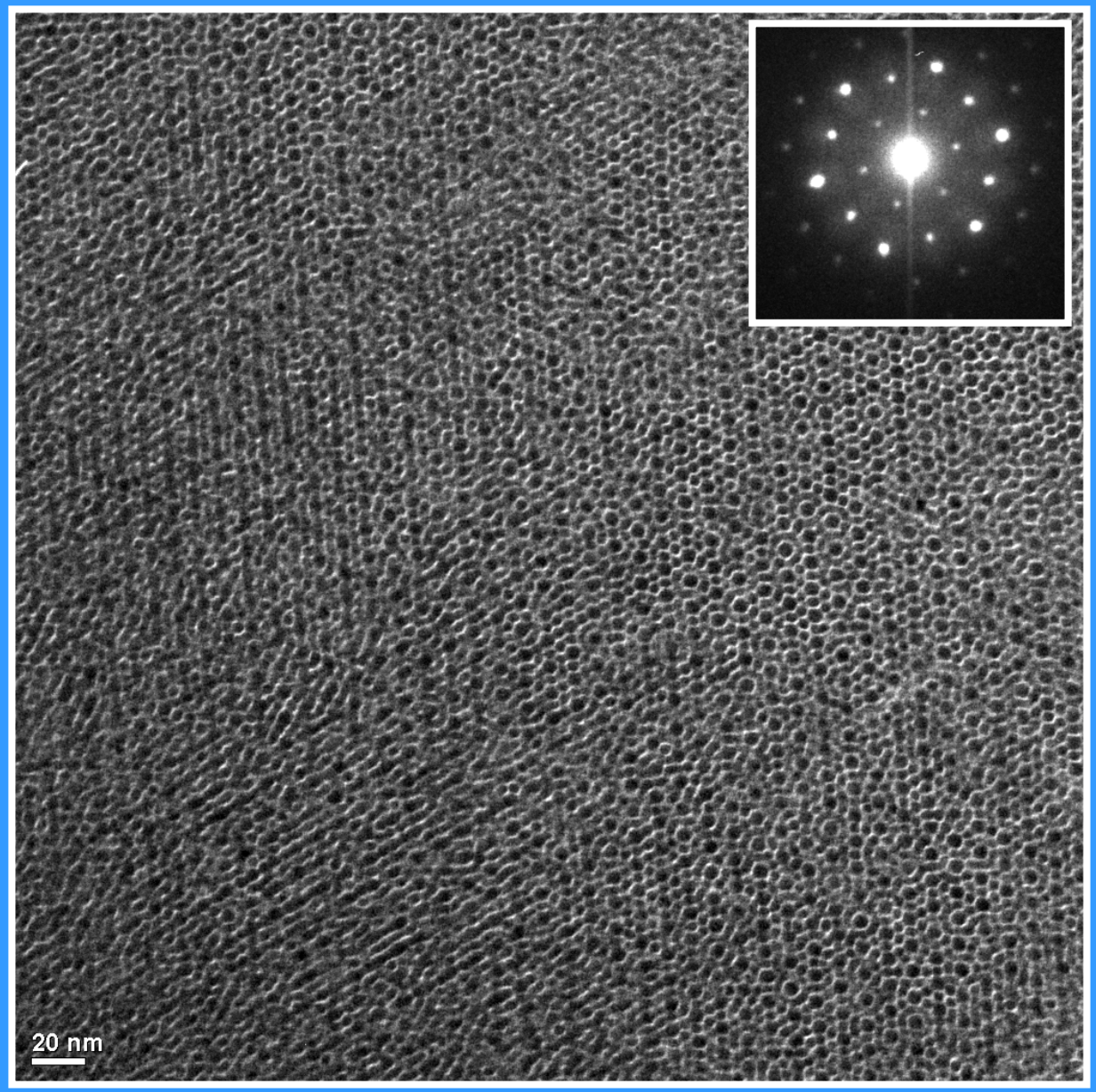

PbSe – Ag binary nanoparticle mixture

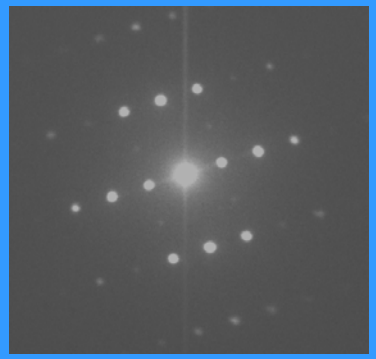

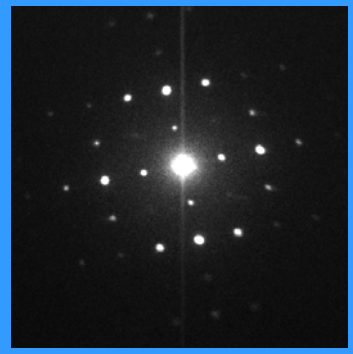

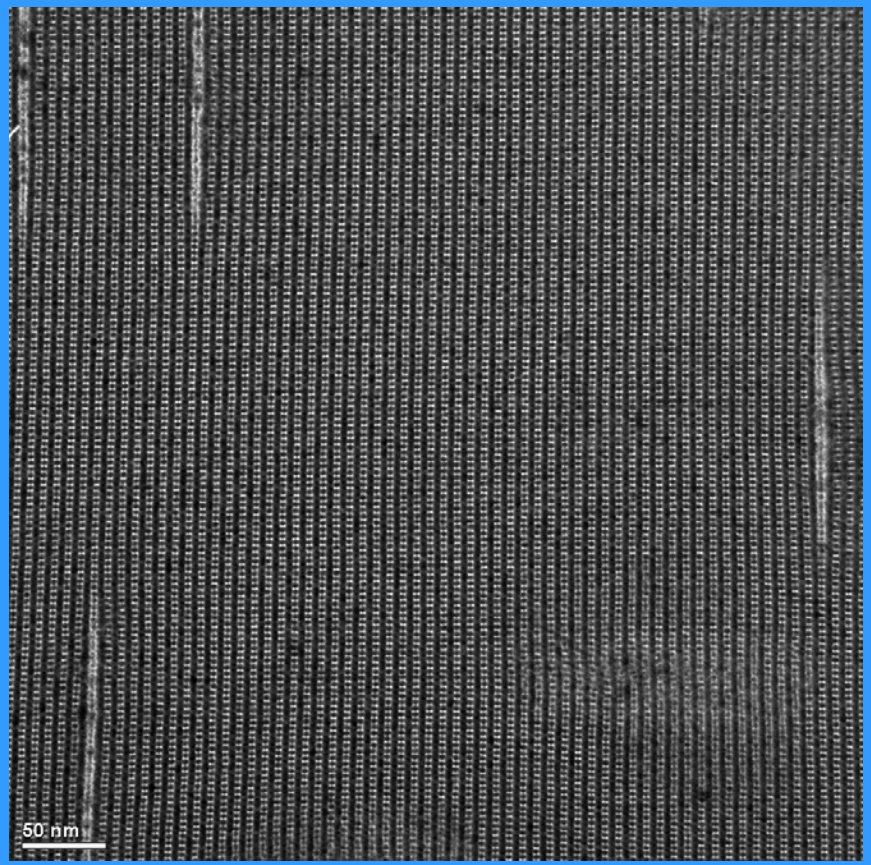

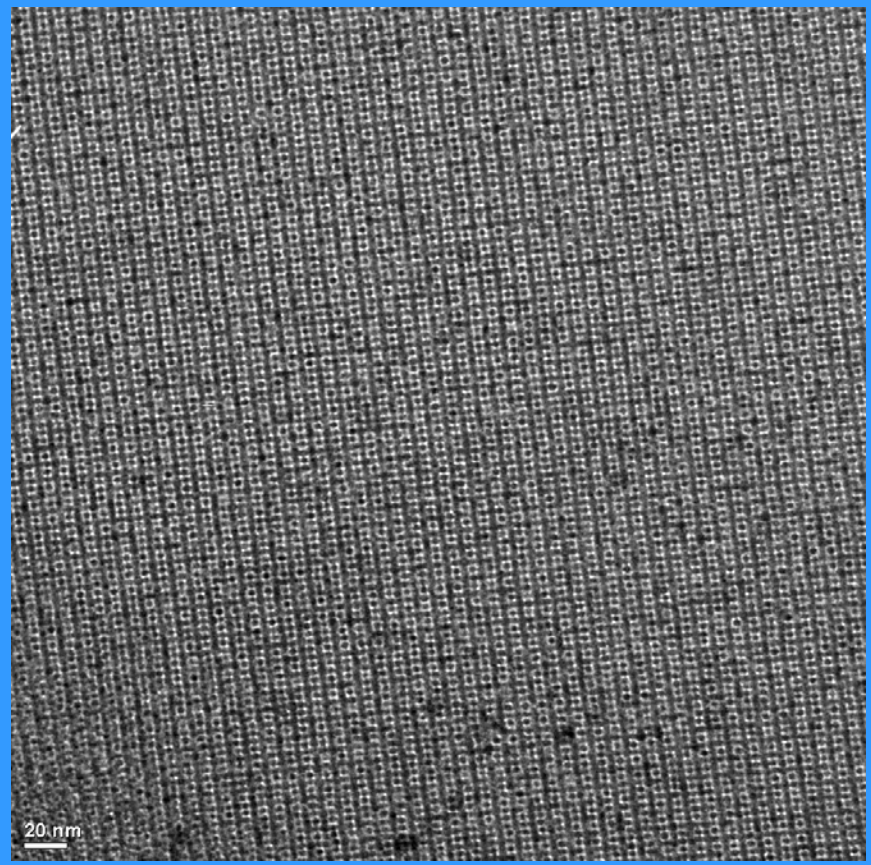

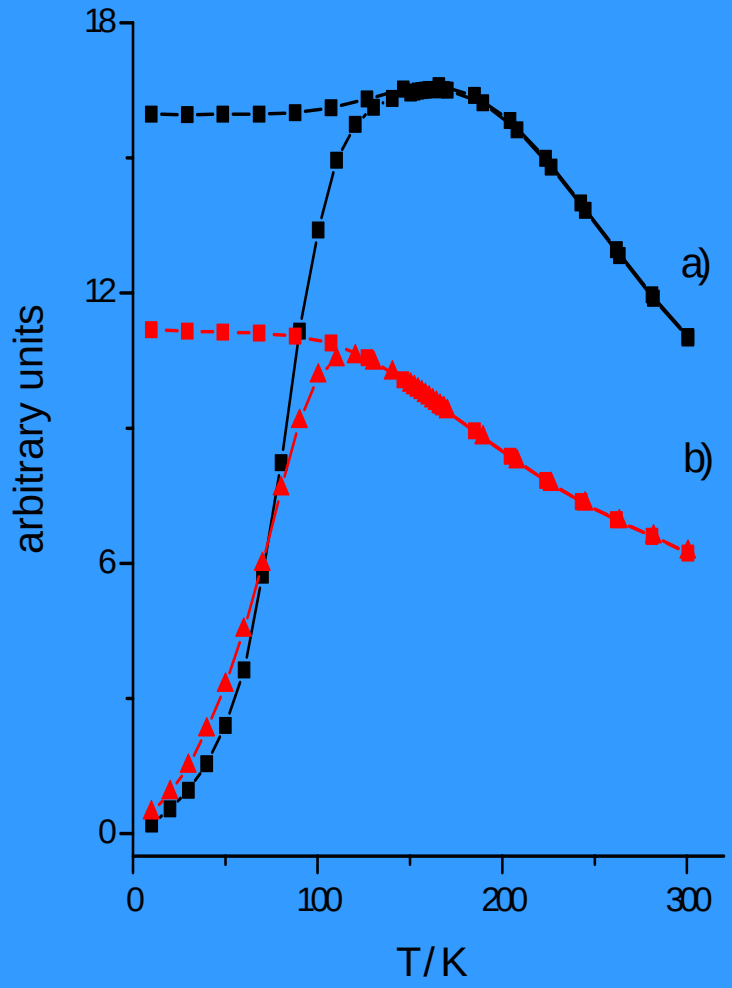
arbitrary units
T / K
a)
b)
0
6
12
18
0
100
200
300

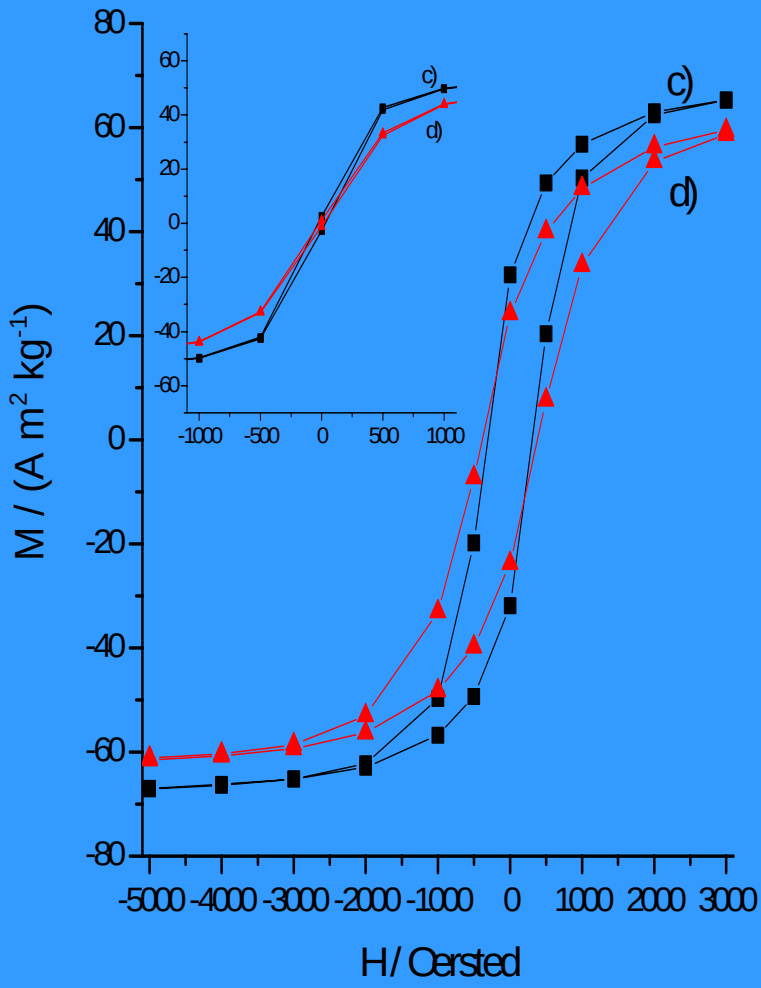
M / (A m2 kg-1)
H / Oersted
c)
d)
80
60
40
20
0
-20
-40
-60
-80
-5000
-4000
-3000
-2000
-1000
0
1000
2000
3000

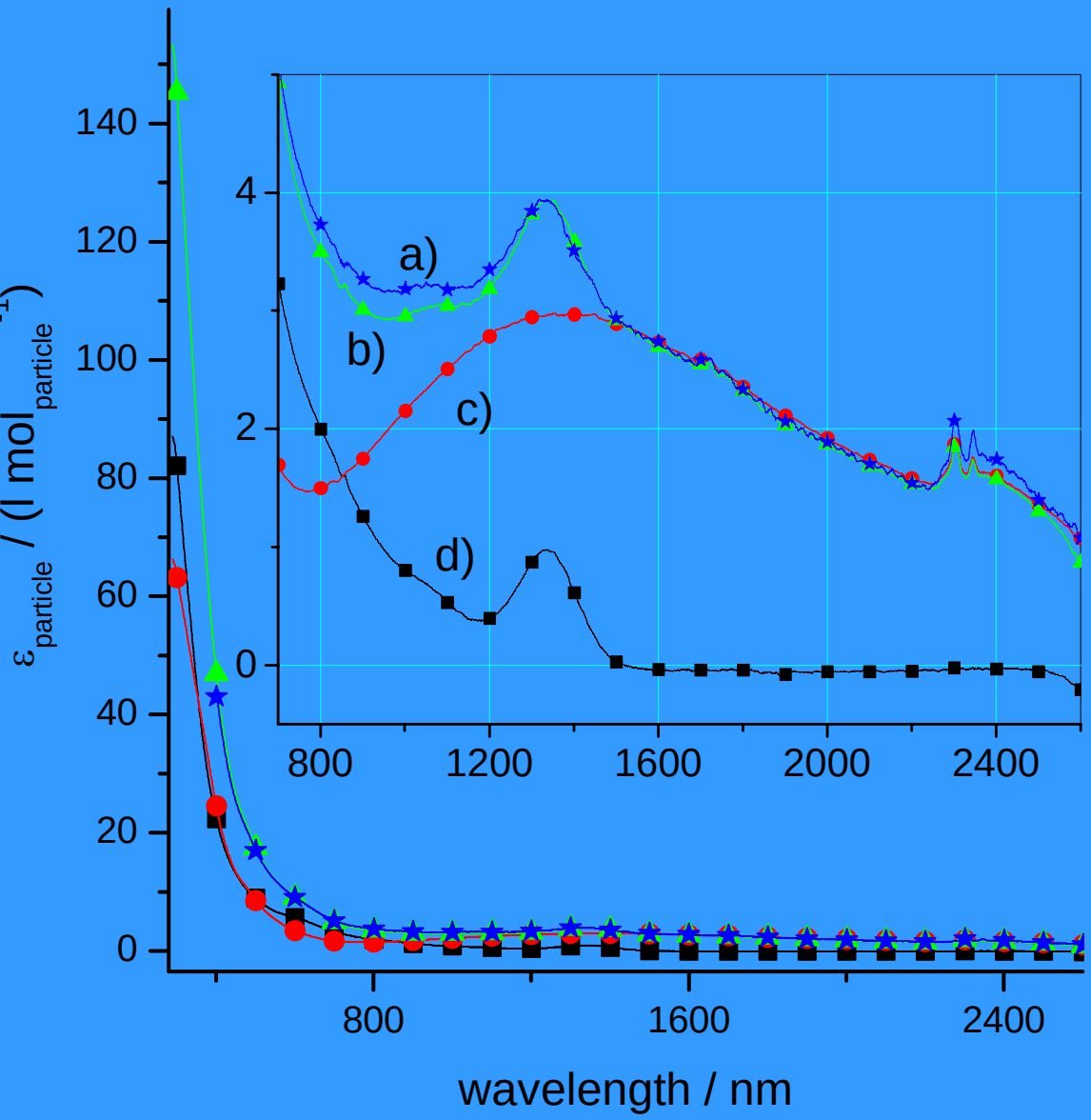
140
120
100
80
60
40
20
0
800
1600
2400
wavelength / nm
ε particle / (l mol particle -1)
4
2
0
800
1200
1600
2000
2400
a)
b)
c)
d)

Complex Compostions and Multi-Component Structures

Simultaneous Reaction
A & B Compounds & Alloys

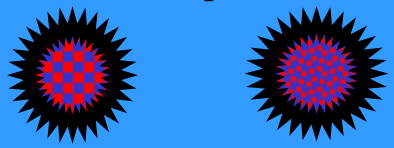

Ferromagnets,
Noble Metals,
Semiconductor QDots,
Ferroelectrics,
Superconductors

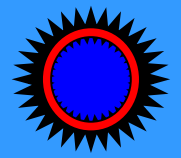

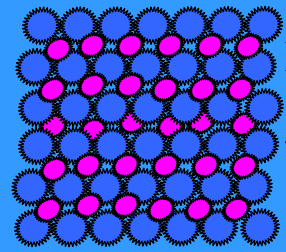

Binary Assembly
AB_2 & AB_{13}

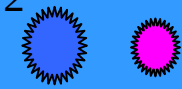

Anneal to remove Organic

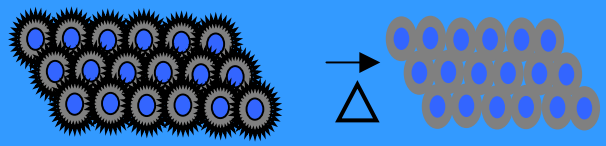

Customize organic linkers (molecular wires)

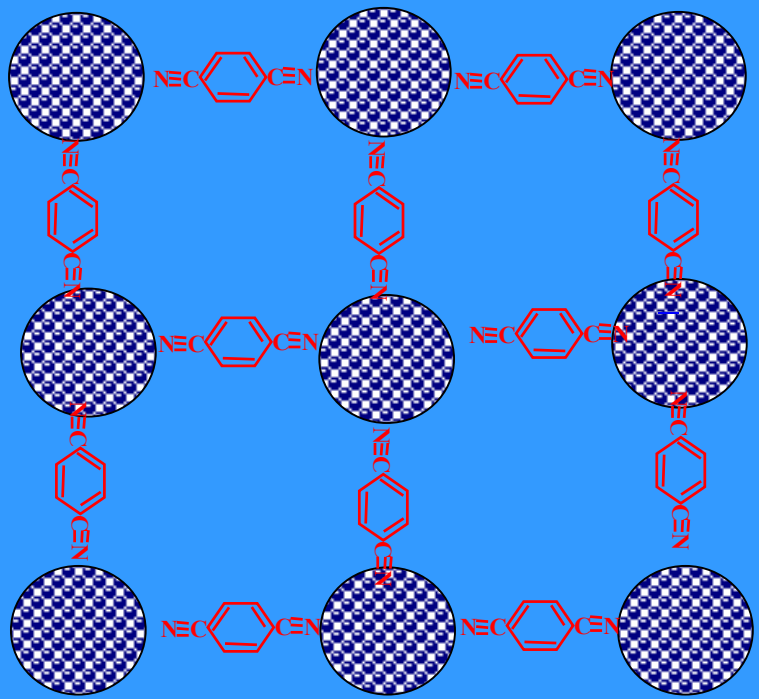

Dicyanobenzene linked Cobalt Nanocrystals